10. SPECIAL TOPICS

In Chap. 1 we learned the basic mathematical tools and physical concepts of vectors and fields. In Chaps. 2 and 3 we learned the fundamental laws of electromagnetics, namely, Maxwell's equations, first in integral form and then in differential form. Then in Chaps. 4 through 9 we studied the elements of their engineering applications which comprised the topics of propagation, transmission, and radiation of electromagnetic waves, and static and quasi-static fields.

This final chapter is devoted to seven independent topics that are based on Chaps. 4 through 9, in that order. The first six topics can be studied separately following the respective chapters. The seventh topic can be studied following Chaps. 8 and 9. These special topics, although independent of each other, have the common goal of extending the knowledge gained in the corresponding previous chapter for the purpose of illustrating a related phenomenon, or application, or technique.

10.1 WAVE PROPAGATION IN IONIZED MEDIUM

In Chap. 4 we studied uniform plane wave propagation in free space. In this section we shall extend the discussion to wave propagation in ionized medium. An example of ionized medium is the earth's ionosphere which is a region of the upper atmosphere extending from approximately 50 km to more than 1000 km above the earth. In this region the constituent gases are ionized, mostly because of ultraviolet radiation from the sun, thereby resulting in the production of positive ions and electrons that are free to move under the influence of the fields of a wave incident upon the medium. The positive ions are, however, heavy compared to electrons and hence they are relatively immobile. The electron motion produces a current that influences the wave propagation.

In fact, in Sec. 1.5 we considered the motion of a cloud of electrons of uniform density N under the influence of a time-varying electric field

$$\mathbf{E} = E_0 \cos \omega t \, \mathbf{i}_x \tag{10.1}$$

and found that the resulting current density is given by

$$\mathbf{J} = \frac{Ne^2}{m\omega} E_0 \sin \omega t \, \mathbf{i}_x = \frac{Ne^2}{m} \int \mathbf{E} \, dt \tag{10.2}$$

where e and m are the electronic charge and mass, respectively. This result is based on the mechanism of continuous acceleration of the electrons by the force due to the applied electric field. In the case of the ionized medium, the electron motion is, however, impeded by the collisions of the electrons with the heavy particles and other electrons. We shall ignore these collisions as well as the negligible influence of the magnetic field associated with the wave.

Considering uniform plane wave propagation in the z direction in an unbounded ionized medium, and with the electric field oriented in the x direction, we then have

$$\frac{\partial E_x}{\partial z} = -\frac{\partial B_y}{\partial t} = -\mu_0 \frac{\partial H_y}{\partial t} \tag{10.3a}$$

$$\frac{\partial H_y}{\partial z} = -J_x - \frac{\partial D_x}{\partial t} = -\frac{Ne^2}{m} \int E_x \, dt - \epsilon_0 \frac{\partial E_x}{\partial t} \tag{10.3b}$$

Differentiating (10.3a) with respect to z and then substituting for $\partial H_y/\partial z$ from (10.3b), we obtain the wave equation

$$\frac{\partial^2 E_x}{\partial z^2} = -\mu_0 \frac{\partial}{\partial t}\left[-\frac{Ne^2}{m}\int E_x\, dt - \epsilon_0 \frac{\partial E_x}{\partial t}\right]$$

$$= \frac{\mu_0 Ne^2}{m} E_x + \mu_0 \epsilon_0 \frac{\partial^2 E_x}{\partial t^2} \tag{10.4}$$

Substituting

$$E_x = E_0 \cos(\omega t - \beta z) \tag{10.5}$$

corresponding to the uniform plane wave solution into (10.4) and simplifying, we get

$$\beta^2 = \omega^2 \mu_0 \epsilon_0 - \frac{\mu_0 Ne^2}{m}$$

$$= \omega^2 \mu_0 \epsilon_0 \left(1 - \frac{Ne^2}{m\epsilon_0 \omega^2}\right) \tag{10.6}$$

Thus the phase constant for propagation in the ionized medium is given by

$$\beta = \omega \sqrt{\mu_0 \epsilon_0 \left(1 - \frac{Ne^2}{m\epsilon_0 \omega^2}\right)} \tag{10.7}$$

This result indicates that the ionized medium behaves as through the permittivity of free space is modified by the multiplying factor $\left(1 - \frac{Ne^2}{m\epsilon_0\omega^2}\right)$. We may therefore write

$$\beta = \omega \sqrt{\mu_0 \epsilon_{\text{eff}}} \tag{10.8}$$

where

$$\epsilon_{\text{eff}} = \epsilon_0 \left(1 - \frac{Ne^2}{m\epsilon_0 \omega^2}\right) \tag{10.9}$$

is the "effective permittivity" of the ionized medium. We note that for $\omega \to \infty$, $\epsilon_{\text{eff}} \to \epsilon_0$ and the medium behaves just as free space. This is to be expected since (10.2) indicates that for $\omega \to \infty$, $\mathbf{J} \to 0$. As ω decreases from ∞, ϵ_{eff} becomes less and less until for ω equal to $\sqrt{Ne^2/m\epsilon_0}$, ϵ_{eff} becomes zero. Hence for $\omega > \sqrt{Ne^2/m\epsilon_0}$, ϵ_{eff} is positive, β is real, and the solution for the electric field remains to be that of a propagating wave. For $\omega < \sqrt{Ne^2/m\epsilon_0}$, ϵ_{eff} is negative, β becomes imaginary, and the solution for the electric field corresponds to no propagation.

Thus waves of frequency $f > \sqrt{Ne^2/4\pi^2 m\epsilon_0}$ propagate in the ionized medium and waves of frequency $f < \sqrt{Ne^2/4\pi^2 m\epsilon_0}$ do not propagate. The quantity $\sqrt{Ne^2/4\pi^2 m\epsilon_0}$ is known as the "plasma frequency" and is denoted by the symbol, f_N. Substituting values for e, m, and ϵ_0, we get

$$f_N = \sqrt{80.6N} \text{ Hz} \tag{10.10}$$

where N is in electrons per meter cubed. We can now write ϵ_{eff} as

$$\epsilon_{\text{eff}} = \epsilon_0\left(1 - \frac{f_N^2}{f^2}\right) \tag{10.11}$$

Proceeding further, we obtain the phase velocity for the propagating range of frequencies, that is, for $f > f_N$, to be

$$v_p = \frac{1}{\sqrt{\mu_0\epsilon_{\text{eff}}}} = \frac{1}{\sqrt{\mu_0\epsilon_0(1 - f_N^2/f^2)}}$$

$$= \frac{c}{\sqrt{1 - f_N^2/f^2}} \tag{10.12}$$

where $c = 1/\sqrt{\mu_0\epsilon_0}$ is the velocity of light in free space. From (10.12), we observe that $v_p > c$ and is a function of the wave frequency. The fact that $v_p > c$ is not a violation of the principle of relativity since the dispersive nature of the medium resulting from the dependence of v_p upon f ensures that information always travels with a velocity less than c (see Sec. 7.4).

To apply what we have learned above concerning propagation in an ionized medium to the case of the earth's ionosphere, we first provide a brief description of the ionosphere. A typical distribution of the ionospheric electron density versus height above the earth is shown in Fig. 10.1. The electron

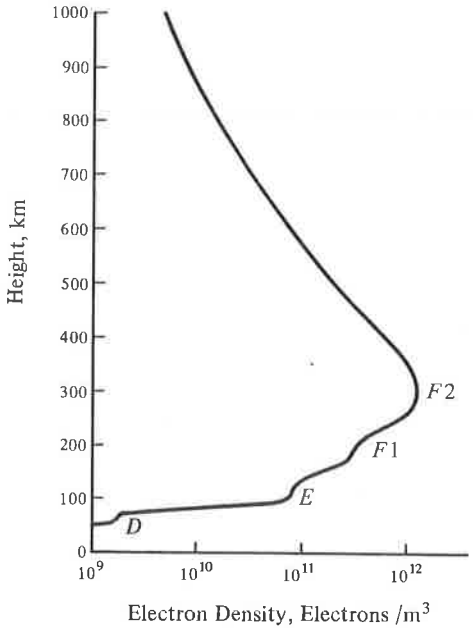

Figure 10.1. A typical distribution of ionospheric electron density versus height above the earth.

density exists in the form of several layers known as D, E, and F layers in which the ionization changes with the hour of the day, the season, the sunspot cycle, and the geographic location. The nomenclature behind the designation of the letters for the layers is due to Appleton in England who in 1925 and at about the same time as Breit and Tuve in the United States demonstrated experimentally the reflection of radio waves by the ionosphere. In his early work, Appleton was accustomed to writing E for the electric field of the wave reflected from the first layer he recognized. Later, when he recognized a second layer, at a greater height, he wrote F for the field of the wave reflected from it. Still later he conjectured that there might be a third layer lower from either of the first two and thus he decided to name the possible lower layer D, thereby leaving earlier letters of the alphabet for other possible undiscovered, still lower layers. Electrons were indeed detected later in the D region.

The D region extends over the altitude range of about 50 km to about 90 km. Since collisions between electrons and heavy particles cannot be neglected in this region, it is mainly an absorbing region. The E region extends from about 90 km to about 150 km. Diurnal and seasonal variations of the E layer electron density are strongly correlated with the zenith angle of the sun. In the F region the lower of the two strata is designated as the $F1$ layer and the higher, more intense ionized stratum is designated as the $F2$ layer. The $F1$ ledge is usually located between 160 km and 200 km. Above this region the $F2$ layer electron density increases with altitude, reaching a peak at a height generally lying between 250 km and 400 km. Above this peak the electron density decreases monotonically with altitude. The $F1$ ledge is present only during the day. During the night the $F1$ and $F2$ layers are identified as a single F layer. The $F2$ layer is the most important from the point of view of radio communication since it contains the greatest concentration of electrons. Paradoxically, it also exhibits several anomalies.

Wave propagation in the ionosphere is complicated by the presence of the earth's magnetic field. If we neglect the earth's magnetic field, then for a wave of frequency f incident vertically on the ionosphere from a transmitter on the ground, it is evident from the propagation condition $f > f_N$ that the wave propagates up to the height at which $f = f_N$ and since it cannot propagate beyond that height, it gets reflected at that height. Thus waves of frequencies less than the maximum plasma frequency corresponding to the peak of the $F2$ layer cannot penetrate the ionosphere. Hence for communication with satellites orbiting above the peak of the ionosphere, frequencies greater than this maximum plasma frequency, also known as the "critical frequency," must be employed. While this critical frequency is a function of the time of day, the season, the sunspot cycle, and the geographic location, it is not greater than about 15 MHz and can be as low as a few megahertz. For a wave incident obliquely on the ionosphere, reflection is possible for frequencies

greater than the critical frequency, up to about three times its value. Hence for earth-to-satellite communication, frequencies generally exceeding about 40 MHz are employed. Lower frequencies permit long-distance, ground-to-ground communication via reflections from the ionospheric layers. This mode of propagation is familiarly known as the "sky wave mode" of propagation. For very low frequencies of the order of several kilohertz and less, the lower boundary of the ionosphere and the earth form a waveguide, thereby permitting waveguide mode of propagation.

In Sec. 4.5 we learned that Doppler shift of frequency occurs when the source or the observer is in motion. Doppler shift can also occur for the case of fixed source and observer if the medium in which the wave propagates is changing with time. The ionosphere provides an example of this phenomenon. For simplicity, let us consider a hypothetical plane slab ionosphere of thickness s and having uniform electron density N. Then for a uniform plane wave of frequency ω propagating normal to the slab, the phase shift undergone by the wave in the thickness of the slab is given by

$$\phi = \omega t - \beta s = \omega t - \omega\sqrt{\mu_0\epsilon_0\left(1 - \frac{Ne^2}{m\epsilon_0\omega^2}\right)}s$$

$$= \omega t - \frac{\omega s}{c}\sqrt{1 - \frac{80.6N}{f^2}} \tag{10.13}$$

If the electron density is now varying with time, the rate of change of phase with time is given by

$$\frac{d\phi}{dt} = \omega + \frac{40.3\,\omega s}{cf^2}\left(1 - \frac{80.6N}{f^2}\right)^{-1/2}\frac{dN}{dt} \tag{10.14}$$

Thus the Doppler shift in the frequency is

$$\omega_D = \frac{40.3\,\omega s}{cf^2}\left(1 - \frac{80.6N}{f^2}\right)^{-1/2}\frac{dN}{dt}$$

or

$$f_D = \frac{40.3s}{cf}\left(1 - \frac{80.6N}{f^2}\right)^{-1/2}\frac{dN}{dt} \tag{10.15}$$

The Doppler shift introduced by the changing ionosphere can be a source of error in satellite navigational systems based on the Doppler shift due to the moving satellite. It is, however, one of the tools for studying the ionosphere.

In this section we learned that in an ionized medium, wave propagation occurs only for frequencies exceeding the plasma frequency corresponding to the electron density. Applying this to the case of the earth's ionosphere, we found that this imposes a lower limit in frequency for communication with

satellites. We also extended the discussion of Doppler shift to the case of a time-varying propagation medium.

REVIEW QUESTIONS

10.1. What is an ionized medium? What influences wave propagation in an ionized medium?

10.2. Provide physical explanation for the frequency dependence of the effective permittivity of an ionized medium.

10.3. Discuss the condition for propagation in an ionized medium.

10.4. What is plasma frequency? How is it related to the electron density?

10.5. Provide a brief description of the earth's ionosphere and discuss how it affects communication.

10.6. Discuss the phenomenon of Doppler shift due to a time-varying medium.

PROBLEMS

10.1. Assume the ionosphere to be represented by a parabolic distribution of electron density as given by

$$N(h) = \frac{10^{14}}{80.6}\left[1 - \left(\frac{h - 300}{100}\right)^2\right] \text{ el/m}^3 \qquad \text{for } 200 < h < 400$$

where h is the height above the ground in kilometers. (a) Find the height at which a vertically incident wave of frequency 8 MHz is reflected. (b) Find the frequency of a vertically incident wave which gets reflected at a height of 220 km. (c) What is the lowest frequency below which communication is not possible across the peak of the layer?

10.2. For a uniform plane wave of frequency 10 MHz propagating normal to a slab of ionized medium of thickness 50 km and uniform plasma frequency 8 MHz, find (a) the phase velocity in the slab, (b) the wavelength in the slab, and (c) the number of wavelengths undergone by the wave in the slab.

10.3. For a uniform plane wave propagating normal to a hypothetical slab ionosphere of thickness 100 km and uniform electron density $(10^{14}/80.6)$ el/m^3, changing with time at the rate of 10^8 el/m^3/s, find the Doppler shift in frequency for (a) $f = 10.1$ MHz and (b) $f = 40$ MHz.

10.4. If you have studied Sec. 7.4, you should be able to show that the group velocity for propagation in the ionized medium is given by

$$v_g = c\sqrt{1 - \frac{f_N^2}{f^2}}$$

Show that for a hypothetical slab ionosphere of thickness s and uniform plasma frequency f_N, a narrow-band modulated signal of carrier frequency $f \gg f_N$ propagating normal to the slab undergoes a time delay in excess of that of the free space value by the amount $f_N^2 s/2cf^2$.

10.2 WAVE PROPAGATION IN ANISOTROPIC MEDIUM

In Sec. 5.2 we learned that for certain dielectric materials known as "anisotropic dielectric materials," **D** is not in general parallel to **E** and the relationship between **D** and **E** is expressed by means of a permittivity tensor consisting of a 3×3 matrix. Similarly, in Sec. 5.3 we learned of the anisotropic property of certain magnetic materials. There are several important applications based on wave propagation in anisotropic materials. A general treatment is, however, very complicated. Hence we shall consider two simple cases.

For the first example, we consider an anisotropic dielectric medium characterized by the **D** to **E** relationship given by

$$\begin{bmatrix} D_x \\ D_y \\ D_z \end{bmatrix} = \begin{bmatrix} \epsilon_{xx} & 0 & 0 \\ 0 & \epsilon_{yy} & 0 \\ 0 & 0 & \epsilon_{zz} \end{bmatrix} \begin{bmatrix} E_x \\ E_y \\ E_z \end{bmatrix} \tag{10.16}$$

and having the permeability μ_0. This simple form of permittivity tensor can be achieved in certain anisotropic liquids and crystals by an appropriate choice of the coordinate system. It is easy to see that the characteristic polarizations for this case are all linear directed along the coordinate axes and having the effective permittivities ϵ_{xx}, ϵ_{yy}, and ϵ_{zz} for the x-, y-, and z-directed polarizations, respectively. Let us consider a uniform plane wave propagating in the z direction. The wave will generally contain both x and y components of the fields. It can be decomposed into two waves, one having an x-directed electric field and the other having a y-directed electric field. These component waves travel individually in the anisotropic medium as though it is isotropic but with different phase velocities since the effective permittivities are different. In view of this, the phase relationship between the two waves, and hence the polarization of the composite wave, changes with distance along the direction of propagation.

To illustrate the foregoing discussion quantitatively, let us consider the electric field of the wave to be linearly polarized at $z = 0$ as given by

$$\mathbf{E}(0) = (E_{x0}\mathbf{i}_x + E_{y0}\mathbf{i}_y) \cos \omega t \tag{10.17}$$

Then assuming (+) wave only, the electric field at an arbitrary value of z is

given by

$$\mathbf{E}(z) = E_{x0} \cos(\omega t - \beta_1 z)\,\mathbf{i}_x + E_{y0} \cos(\omega t - \beta_2 z)\,\mathbf{i}_y \tag{10.18}$$

where

$$\beta_1 = \omega\sqrt{\mu_0 \epsilon_{xx}} \tag{10.19a}$$

$$\beta_2 = \omega\sqrt{\mu_0 \epsilon_{yy}} \tag{10.19b}$$

are the phase constants corresponding to the x-polarized and y-polarized component waves, respectively. Thus the phase difference between the x and y components of the field is given by

$$\Delta\phi = (\beta_2 - \beta_1)z \tag{10.20}$$

As the composite wave progresses along the z direction, $\Delta\phi$ changes from zero at $z = 0$ to $\pi/2$ at $z = \pi/2(\beta_2 - \beta_1)$ to π at $z = \pi/(\beta_2 - \beta_1)$, and so on. The polarization of the composite wave thus changes from linear at $z = 0$ to elliptical for $z > 0$, becoming linear again at $z = \pi/(\beta_2 - \beta_1)$, but rotated by an angle of $2 \tan^{-1}(E_{y0}/E_{x0})$, as shown in Fig. 10.2. Thereafter, it becomes elliptical again, returning back to the original linear polarization at $z = 2\pi/(\beta_2 - \beta_1)$, and so on.

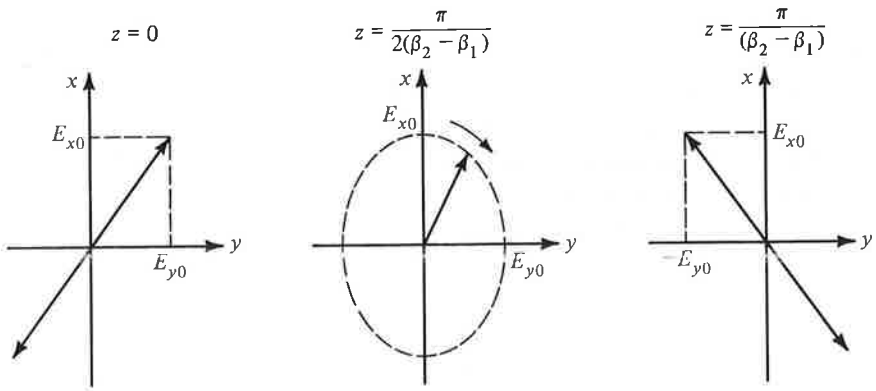

Figure 10.2. The change in polarization of the field of a wave propagating in the anisotropic dielectric medium characterized by Eq. (10.16).

For the second example, we consider propagation in a ferrite medium. Ferrites are a class of magnetic materials which when subject to a d.c. magnetizing field exhibit anisotropic magnetic properties. Since there are phase differences associated with the relationships between the components of **B** and the components of **H** due to this anisotropy, it is convenient to use the phasor notation and write the relationship in terms of the phasor components. For an applied d.c. magnetic field along the direction of propagation of the

wave, which we assume to be the z direction, this relationship is given by

$$\begin{bmatrix} \bar{B}_x \\ \bar{B}_y \\ \bar{B}_z \end{bmatrix} = \begin{bmatrix} \mu & -j\kappa & 0 \\ j\kappa & \mu & 0 \\ 0 & 0 & \mu_0 \end{bmatrix} \begin{bmatrix} \bar{H}_x \\ \bar{H}_y \\ \bar{H}_z \end{bmatrix} \tag{10.21}$$

where μ and κ depend upon the material, the strength of the d.c. magnetic field, and the wave frequency.

To find the characteristic polarizations, we first note from (10.21) that

$$\bar{B}_x = \mu \bar{H}_x - j\kappa \bar{H}_y \tag{10.22a}$$

$$\bar{B}_y = j\kappa \bar{H}_x + \mu \bar{H}_y \tag{10.22b}$$

Setting $\bar{B}_x/\bar{B}_y$ equal to $\bar{H}_x/\bar{H}_y$, we then have

$$\frac{\mu \bar{H}_x - j\kappa \bar{H}_y}{j\kappa \bar{H}_x + \mu \bar{H}_y} = \frac{\bar{H}_x}{\bar{H}_y}$$

which upon solution for $\bar{H}_x/\bar{H}_y$ gives

$$\frac{\bar{H}_x}{\bar{H}_y} = \pm j \tag{10.23}$$

This result corresponds to equal amplitudes of H_x and H_y and phase difference of $\pm 90°$. Thus the characteristic polarizations are both circular, rotating in opposite senses as viewed along the z direction.

The effective permeabilities of the ferrite medium corresponding to the characteristic polarizations are

$$\begin{aligned} \frac{\bar{B}_x}{\bar{H}_x} &= \frac{\mu \bar{H}_x - j\kappa \bar{H}_y}{\bar{H}_x} \\ &= \mu - j\kappa \frac{\bar{H}_y}{\bar{H}_x} \\ &= \mu \mp \kappa \qquad \text{for } \frac{\bar{H}_x}{\bar{H}_y} = \pm j \end{aligned} \tag{10.24}$$

The phase constants associated with the propagation of the characteristic waves are

$$\beta_\pm = \omega \sqrt{\epsilon(\mu \mp \kappa)} \tag{10.25}$$

where the subscripts $+$ and $-$ refer to $\bar{H}_x/\bar{H}_y = +j$ and $\bar{H}_x/\bar{H}_y = -j$, respectively. We note from (10.25) that β_+ can become imaginary if $(\mu - \kappa) < 0$. When this happens, wave propagation does not occur for that characteristic

polarization. We shall hereafter assume that the wave frequency is such that both characteristic waves propagate.

Let us now consider the magnetic field of the wave to be linearly polarized in the x direction at $z = 0$, that is,

$$\mathbf{H}(0) = H_0 \cos \omega t \, \mathbf{i}_x \tag{10.26}$$

Then we can express (10.26) as the superposition of two circularly polarized fields having opposite senses of rotation in the xy plane in the manner

$$\begin{aligned}\mathbf{H}(0) = &\left(\frac{H_0}{2} \cos \omega t \, \mathbf{i}_x + \frac{H_0}{2} \sin \omega t \, \mathbf{i}_y\right) \\ &+ \left(\frac{H_0}{2} \cos \omega t \, \mathbf{i}_x - \frac{H_0}{2} \sin \omega t \, \mathbf{i}_y\right)\end{aligned} \tag{10.27}$$

The circularly polarized field inside the first pair of parentheses on the right side of (10.27) corresponds to

$$\frac{\bar{H}_x}{\bar{H}_y} = \frac{H_0/2}{-jH_0/2} = +j$$

whereas that inside the second pair of parentheses corresponds to

$$\frac{\bar{H}_x}{\bar{H}_y} = \frac{H_0/2}{jH_0/2} = -j$$

Assuming propagation in the positive z direction, the field at an arbitrary value of z is then given by

$$\begin{aligned}\mathbf{H}(z) = &\left[\frac{H_0}{2} \cos (\omega t - \beta_+ z) \, \mathbf{i}_x + \frac{H_0}{2} \sin (\omega t - \beta_+ z) \, \mathbf{i}_y\right] \\ &+ \left[\frac{H_0}{2} \cos (\omega t - \beta_- z) \, \mathbf{i}_x - \frac{H_0}{2} \sin (\omega t - \beta_- z) \, \mathbf{i}_y\right] \\ = &\left[\frac{H_0}{2} \cos \left(\omega t - \frac{\beta_+ + \beta_-}{2} z - \frac{\beta_+ - \beta_-}{2} z\right) \mathbf{i}_x\right. \\ &\left. + \frac{H_0}{2} \sin \left(\omega t - \frac{\beta_+ + \beta_-}{2} z - \frac{\beta_+ - \beta_-}{2} z\right) \mathbf{i}_y\right] \\ &+ \left[\frac{H_0}{2} \cos \left(\omega t - \frac{\beta_+ + \beta_-}{2} z + \frac{\beta_+ - \beta_-}{2} z\right) \mathbf{i}_x\right. \\ &\left. - \frac{H_0}{2} \sin \left(\omega t - \frac{\beta_+ + \beta_-}{2} z + \frac{\beta_+ - \beta_-}{2} z\right) \mathbf{i}_y\right] \\ = &\left[H_0 \cos \left(\frac{\beta_- - \beta_+}{2} z\right) \mathbf{i}_x + H_0 \sin \left(\frac{\beta_- - \beta_+}{2} z\right) \mathbf{i}_y\right] \\ &\cdot \cos \left(\omega t - \frac{\beta_+ + \beta_-}{2} z\right)\end{aligned} \tag{10.28}$$

The result given by (10.28) indicates that the x and y components of the field are in phase at any given value of z. Hence the field is linearly polarized for all values of z. The direction of polarization is, however, a function of z since

$$\frac{H_y}{H_x} = \frac{H_0 \sin [(\beta_- - \beta_+)/2]z}{H_0 \cos [(\beta_- - \beta_+)/2]z} = \tan \frac{\beta_- - \beta_+}{2} z \tag{10.29}$$

and hence the angle made by the field vector with the x axis is $\frac{\beta_- - \beta_+}{2} z$. Thus the direction of polarization rotates linearly with z at a rate of $\frac{\beta_- - \beta_+}{2}$. This phenomenon is known as "Faraday rotation" and is illustrated with the aid of the sketches in Fig. 10.3. The sketches in any given column correspond to a fixed value of z whereas the sketches in a given row correspond to a fixed value of t. At $z = 0$, the field is linearly polarized in the x direction and is the superposition of two counter-rotating circularly polarized fields as shown by the time series of sketches in the first column. If the medium is isotropic, the two counter-rotating circularly polarized fields undergo the same amount of phase lag with z and the field remains linearly polarized in the x direction as shown by the dashed lines in the second and third columns. For the case of the anisotropic medium, the two circularly polarized fields undergo different amounts of phase lag with z. Hence their superposition results in a linear polarization making an angle with the x direction and increasing linearly with z as shown by the solid lines in the second and third columns.

The phenomenon of Faraday rotation in a ferrite medium that we have just discussed forms the basis for a number of devices in the microwave field. The phenomenon itself is not restricted to ferrites. For example, an ionized medium immersed in a d.c. magnetic field possesses anisotropic properties which give rise to Faraday rotation of a linearly polarized wave propagating along the d.c. magnetic field. A natural example of this is propagation along the earth's magnetic field in the ionosphere. A simple modern example of the application of Faraday rotation is, however, illustrated by the magneto-optical switch. In fact, Faraday rotation was originally discovered in the optics regime.

The magneto-optical switch is a device for modulating a laser beam by switching on and off an electric current. The electric current generates a magnetic field that rotates the magnetization vector in a magnetic iron-garnet film on a substrate of garnet, in the plane of the film through which a light wave passes. When it enters the film, the light wave field is linearly polarized normal to the plane of the film. If the current in the electric circuit is off, the

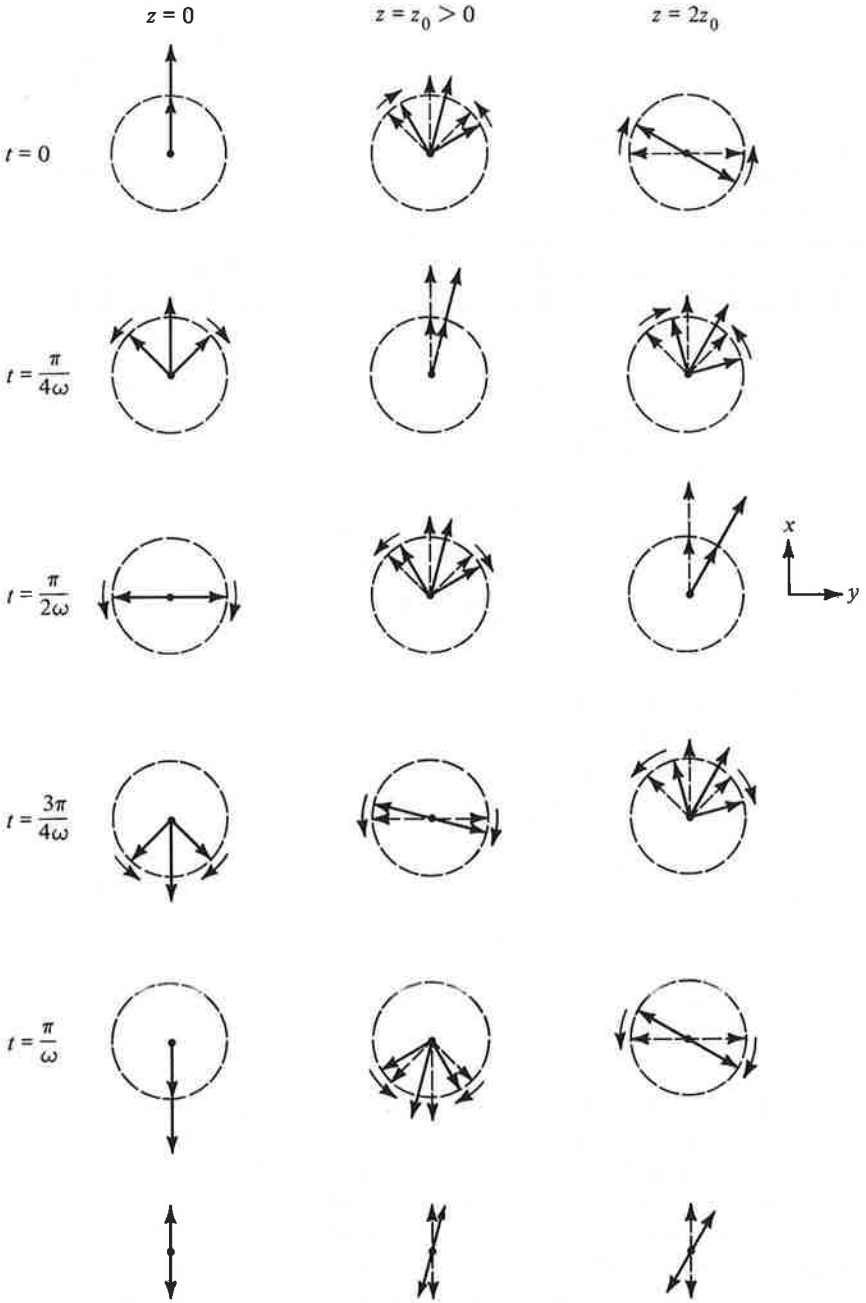

Figure 10.3. For illustrating the phenomenon of Faraday rotation.

magnetization vector is normal to the direction of propagation of the wave and the wave emerges out of the film without change of polarization, as shown in Fig. 10.4(a). If the current in the electric circuit is on, the magnetization vector is parallel to the direction of propagation of the wave, the light wave undergoes Faraday rotation and emerges out of the film with its polarization rotated by 90°, as shown in Fig. 10.4(b). After it emerges out of the film, the light beam is passed through a polarizer which has the property of absorbing light of the original polarization but passing through the light of

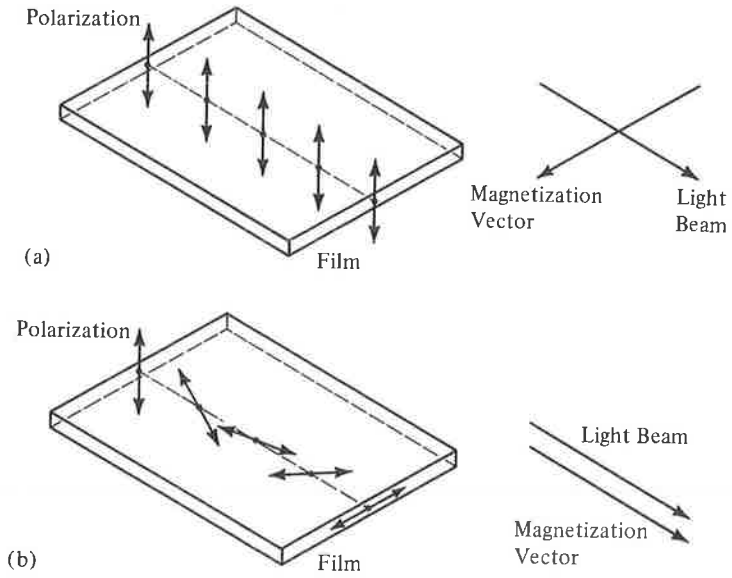

Figure 10.4. For illustrating the principle of operation of a magneto-optical switch.

the 90°-rotated polarization. Thus the beam is made to turn on and off by the switching on and off of the current in the electric circuit. In this manner, any coded message can be made to be carried by the light beam.

In this section we discussed wave propagation in an anisotropic medium. In particular, we learned that in a ferrite medium, a linearly polarized wave propagating along the direction of an applied d.c. magnetic field undergoes Faraday rotation. We then briefly mentioned other examples of media in which Faraday rotation takes place and finally discussed the operation of the magneto-optical switch, a device employing Faraday rotation for modulating a light beam.

REVIEW QUESTIONS

10.7. Discuss the principle behind wave propagation in an anisotropic medium based on the decomposition of the wave into characteristic waves.

10.8. When does a wave propagate in an anisotropic medium without change in polarization?

10.9. What is Faraday rotation? When does Faraday rotation take place in an anisotropic medium?

10.10. Consult appropriate reference books and list three applications of Faraday rotation.

10.11. What is a magneto-optical switch? Discuss its operation.

PROBLEMS

10.5. For the anisotropic medium characterized by the **D** to **E** relationship given by Eq. (10.16), assume $\epsilon_{xx} = 4\epsilon_0$, $\epsilon_{yy} = 9\epsilon_0$, and $\epsilon_{zz} = 2\epsilon_0$, and find the distance in which the phase difference between the x and y components of a plane wave of frequency 10^9 Hz propagating in the z direction changes by the amount π.

10.6. Show that for plane wave propagation in an anisotropic medium, the angle between **E** and **H** is not in general equal to 90°. For the anisotropic dielectric medium of Problem 10.5, find the angle between **E** and **H** for **E** linearly polarized along the bisector of the angle between the x and y axes.

10.7. For a wave of frequency ω, the quantities μ and κ in the permeability matrix of Eq. (10.21) are given by

$$\mu = \mu_0\left[1 + \frac{\omega_0\omega_M}{\omega_0^2 - \omega^2}\right]$$

$$\kappa = -\mu_0\frac{\omega\omega_M}{\omega_0^2 - \omega^2}$$

where $\omega_0 = \mu_0|e|H_0/m$, $\omega_M = \mu_0|e|M_0/m$, H_0 is the d.c. magnetizing field, M_0 is the magnetic dipole moment per unit volume in the material in the absence of the wave, e is the charge of an electron, and m is the mass of an electron. (a) Show that the effective permeabilities corresponding to the characteristic polarizations are $\mu_0\left[1 + \frac{\omega_M}{\omega_0 \mp \omega}\right]$ for $\bar{H}_x/\bar{H}_y = \pm j$. (b) Compute the Faraday rotation angle in degrees per centimeter along the z direction for $\omega = 10^{10}$ rad/s, if $\omega_M = 5 \times 10^{10}$ rad/s, $\omega_0 = 1.5 \times 10^{10}$ rad/s, and $\epsilon = 9\epsilon_0$.

10.8. For the quantities defined in Problem 10.7 for the ferrite medium, show that

for $\omega_0 \ll \omega$ and $\omega_M \ll \omega$, the Faraday rotation per unit distance along the z direction is $\frac{\omega_M}{2}\sqrt{\mu_0\epsilon}$. Compute its value in degrees per centimeter if $\omega_M = 5 \times 10^{10}$ rad/s and $\epsilon = 9\epsilon_0$.

10.3 THE SMITH CHART

In Sec. 6.6 we studied reflection and transmission at the junction of two transmission lines. We found that when a line of certain characteristic impedance is terminated by another line of different characteristic impedance, as shown in Fig. 10.5, standing waves result on the first line. The degree of existence of the standing waves was defined by the standing wave ratio (SWR) which is the ratio of the voltage maximum to the voltage minimum of the standing wave pattern. In this section we shall proceed further and introduce the Smith Chart, which is a useful graphical aid in the solution of transmission-line and many other problems.

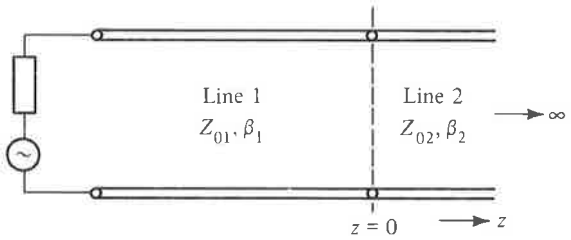

Figure 10.5. A transmission line terminated by another infinitely long transmission line.

First we define the line impedance $\bar{Z}(z)$ at a given value of z on the line as the ratio of the complex line voltage to the complex line current at that value of z, that is,

$$\bar{Z}(z) = \frac{\bar{V}(z)}{\bar{I}(z)} \tag{10.30}$$

From the solutions for the line voltage and line current on line 2 given by (6.71a) and (6.71b), respectively, the line impedance in line 2 is given by

$$\bar{Z}_2(z) = \frac{\bar{V}_2(z)}{\bar{I}_2(z)} = Z_{02}$$

Thus the line impedance at all points on line 2 is simply equal to the characteristic impedance of that line. This is because the line is infinitely long and hence there is only a (+) wave on the line. From the solutions for the line voltage and line current in line 1 given by (6.70a) and (6.70b), respectively,

the line impedance for that line is given by

$$\bar{Z}_1(z) = \frac{\bar{V}_1(z)}{\bar{I}_1(z)} = Z_{01}\frac{\bar{V}_1^+ e^{-j\beta_1 z} + \bar{V}_1^- e^{j\beta_1 z}}{\bar{V}_1^+ e^{-j\beta_1 z} - \bar{V}_1^+ e^{j\beta_1 z}}$$

$$= Z_{01}\frac{1 + \bar{\Gamma}_V(z)}{1 - \bar{\Gamma}_V(z)} \tag{10.31}$$

where

$$\bar{\Gamma}_V(z) = \frac{\bar{V}_1^- e^{j\beta_1 z}}{\bar{V}_1^+ e^{-j\beta_1 z}} = \bar{\Gamma}_V(0)e^{j2\beta_1 z} \tag{10.32}$$

$$\bar{\Gamma}_V(0) = \frac{\bar{V}_1^-}{\bar{V}_1^+} = \frac{Z_{02} - Z_{01}}{Z_{02} + Z_{01}} \tag{10.33}$$

The quantity $\bar{\Gamma}_V(0)$ is the voltage reflection coefficient at the junction $z = 0$ and $\bar{\Gamma}_V(z)$ is the voltage reflection coefficient at any value of z.

To compute the line impedance at a particular value of z, we first compute $\bar{\Gamma}_V(0)$ from a knowledge of Z_{02} which is the terminating impedance to line 1. We then compute $\bar{\Gamma}_V(z) = \bar{\Gamma}_V(0)e^{j2\beta_1 z}$ which is a complex number having the same magnitude as that of $\bar{\Gamma}_V(0)$ but a phase angle equal to $2\beta_1 z$ plus the phase angle of $\bar{\Gamma}_V(0)$. The computed value of $\bar{\Gamma}_V(z)$ is then substituted in (10.31) to find $\bar{Z}_1(z)$. All of this complex algebra is eliminated through the use of the Smith Chart.

The Smith Chart is a mapping of the values of normalized line impedance onto the reflection coefficient ($\bar{\Gamma}_V$) plane. The normalized line impedance $\bar{Z}_n(z)$ is the ratio of the line impedance to the characteristic impedance of the line. From (10.31), and omitting the subscript 1 for the sake of generality, we have

$$\bar{Z}_n(z) = \frac{\bar{Z}(z)}{Z_0} = \frac{1 + \bar{\Gamma}_V(z)}{1 - \bar{\Gamma}_V(z)} \tag{10.34}$$

Conversely,

$$\bar{\Gamma}_V(z) = \frac{\bar{Z}_n(z) - 1}{\bar{Z}_n(z) + 1} \tag{10.35}$$

Writing $\bar{Z}_n = r + jx$ and substituting into (10.35), we find that

$$|\bar{\Gamma}_V| = \left|\frac{r + jx - 1}{r + jx + 1}\right| = \frac{\sqrt{(r-1)^2 + x^2}}{\sqrt{(r+1)^2 + x^2}} \leq 1 \qquad \text{for } r \geq 0$$

Thus, we note that all passive values of normalized line impedances, that is, points in the right half of the complex $\bar{Z}_n$ plane shown in Fig. 10.6(a) are mapped onto the region within the circle of radius unity in the complex $\bar{\Gamma}_V$ plane shown in Fig. 10.6(b).

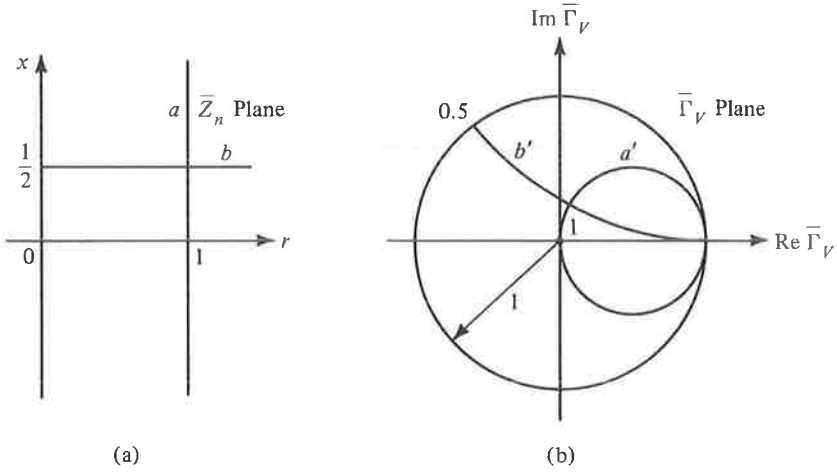

Figure 10.6. For illustrating the development of the Smith Chart.

We can now assign values for $\bar{Z}_n$, compute the corresponding values of $\bar{\Gamma}_V$, and plot them on the $\bar{\Gamma}_V$ plane but indicating the values of $\bar{Z}_n$ instead of the values of $\bar{\Gamma}_V$. To do this in a systematic manner, we consider contours in the $\bar{Z}_n$ plane corresponding to constant values of r, as shown for example by the line marked a for $r = 1$, and corresponding to constant values of x, as shown for example by the line marked b for $x = \frac{1}{2}$ in Fig. 10.6(a).

By considering several points along line a, computing the corresponding values of $\bar{\Gamma}_V$, plotting them on the $\bar{\Gamma}_V$ plane, and joining them, we obtain the contour marked a' in Fig. 10.6(b). Although it can be shown analytically that this contour is a circle of radius $\frac{1}{2}$ and centered at (1/2, 0), it is a simple task to write a computer program to perform this operation, including the plotting. Similarly, by considering several points along line b and following the same procedure, we obtain the contour marked b' in Fig. 10.6(b). Again, it can be shown analytically that this contour is a portion of a circle of radius 2 and centered at (1, 2). We can now identify the points on contour a' as corresponding to $r = 1$ by placing the number 1 beside it and the points on contour b' as corresponding to $x = \frac{1}{2}$ by placing the number 0.5 beside it. The point of intersection of contours a' and b' then corresponds to $\bar{Z}_n = 1 + j0.5$.

When the procedure discussed above is applied to many lines of constant r and constant x covering the entire right half of the $\bar{Z}_n$ plane, we obtain the Smith Chart. In a commercially available form shown in Fig. 10.7, the Smith Chart contains contours of constant r and constant x at appropriate increments of r and x in the range $0 < r < \infty$ and $-\infty < x < \infty$ so that interpolation between the contours can be carried out to a good degree of accuracy.

Let us now consider the transmission line system shown in Fig. 10.8,

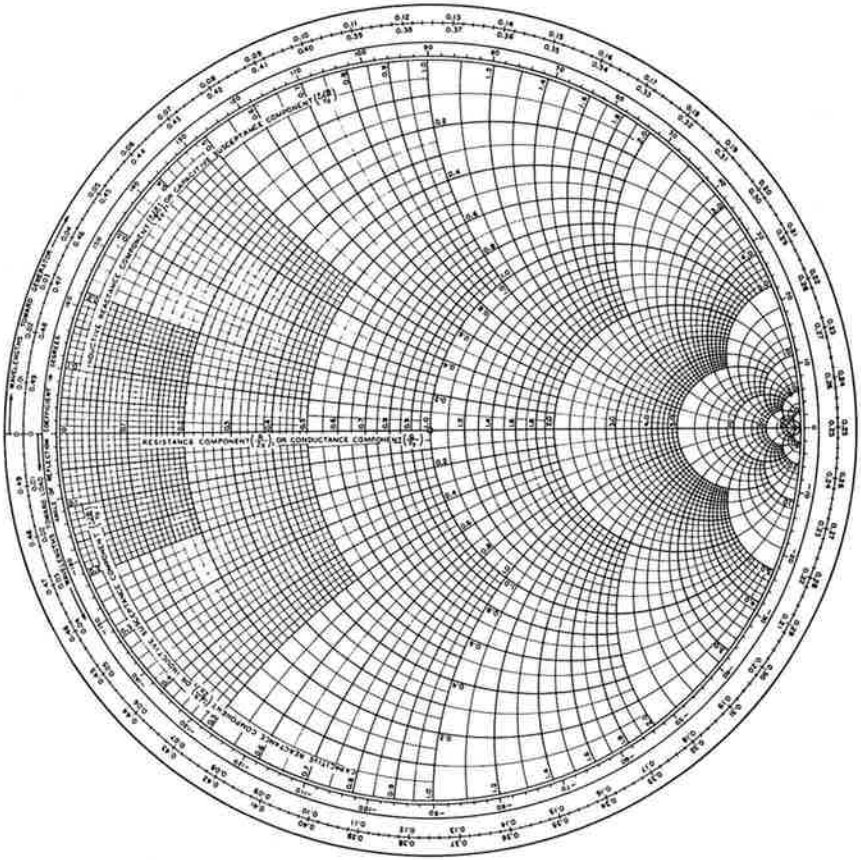

Figure 10.7. A commercially available form of the Smith Chart (copyrighted by and reproduced with the permission of Kay Elemetrics Corp., Pine Brook, N.J.).

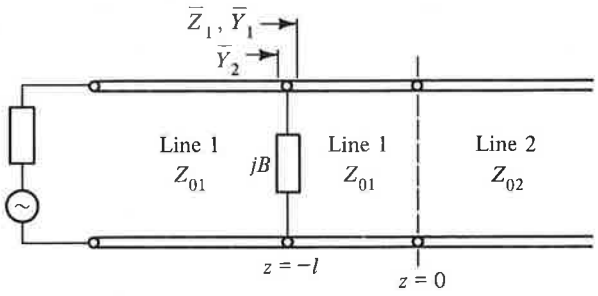

Figure 10.8. A transmission-line system for illustrating the computation of several quantities by using the Smith Chart.

which is the same as that in Fig. 10.5 except that a reactive element having susceptance (reciprocal of reactance) B is connected in parallel with line 1 at a distance l from the junction. Let us assume $Z_{01} = 150$ ohms, $Z_{02} = 50$ ohms, $B = -0.003$ mho, and $l = 0.375\lambda_1$, where λ_1 is the wavelength in line 1 corresponding to the source frequency, and find the following quantities by using the Smith Chart, as shown in Fig. 10.9:

1. $\bar{Z}_1$, line impedance just to the right of jB: First we note that since line 2 is infinitely long, the load for line 1 is simply 50 ohms. Normalizing this with respect to the characteristic impedance of line 1, we obtain the normalized load impedance for line 1 to be

$$\bar{Z}_n(0) = \frac{50}{150} = \frac{1}{3}$$

Locating this on the Smith Chart at point A in Fig. 10.9 amounts to computing the reflection coefficient at the junction, that is, $\bar{\Gamma}_V(0)$. Now the reflection coefficient at $z = -l = -0.375\lambda_1$, being equal to $\bar{\Gamma}_V(0)e^{-j2\beta_1 l} = \bar{\Gamma}_V(0)e^{-j1.5\pi}$, can be located on the Smith Chart by moving A such that the magnitude remains constant but the phase angle decreases by 1.5π. This is equivalent to moving it on a circle with

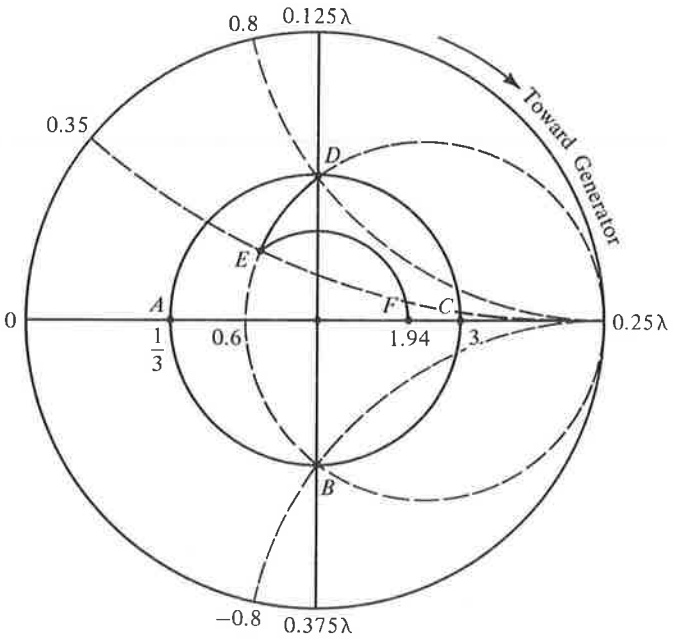

Figure 10.9. For illustrating the use of the Smith Chart in the computation of several quantities for the transmission-line system of Fig. 10.8.

its center at the center of the Smith Chart and in the clockwise direction by 1.5π or 270° so that point B is reached. Actually, it is not necessary to compute this angle since the Smith Chart contains a distance scale in terms of λ along its periphery for movement from load toward generator and vice versa, based on a complete revolution for one-half wavelength. The normalized impedance at point B can now be read off the chart and multiplied by the characteristic impedance of the line to obtain the required impedance value. Thus

$$\bar{Z}_1 = (0.6 - j0.8)150 = (90 - j120) \text{ ohms.}$$

2. SWR on line 1 to the right of jB: From (6.81)

$$\text{SWR} = \frac{1 + |\Gamma_V|}{1 - |\Gamma_V|} = \frac{1 + |\bar{\Gamma}_V|e^{j0}}{1 - |\bar{\Gamma}_V|e^{j0}} \tag{10.36}$$

Comparing the right side of (10.36) with the expression for $\bar{Z}_n$ given by (10.34), we note that it is simply equal to $\bar{Z}_n$ corresponding to phase angle of $\bar{\Gamma}_V$ equal to zero. Thus, to find the SWR, we locate the point on the Smith Chart having the same $|\bar{\Gamma}_V|$ as that for $z = 0$, but having a phase angle equal to zero, that is, the point C in Fig. 10.9, and then read off the normalized resistance value at that point. Here, it is equal to 3 and hence the required SWR is equal to 3. In fact, the circle passing through C and having its center at the center of the Smith Chart is known as the "constant SWR (= 3) circle" since for any normalized load impedance to line 1 lying on that circle, the SWR is the same (and equal to 3).

3. $\bar{Y}_1$, line admittance just to the right of jB: To find this, we note that the normalized line admittance $\bar{Y}_n$ at any value of z, that is, the line admittance normalized with respect to the line characteristic admittance Y_0 (reciprocal of Z_0) is given by

$$\begin{aligned}
\bar{Y}_n(z) &= \frac{\bar{Y}(z)}{Y_0} = \frac{Z_0}{\bar{Z}(z)} = \frac{1}{\bar{Z}_n(z)} \\
&= \frac{1 - \bar{\Gamma}_V(z)}{1 + \bar{\Gamma}_V(z)} = \frac{1 + \bar{\Gamma}_V(z)e^{\pm j\pi}}{1 - \bar{\Gamma}_V(z)e^{\pm j\pi}} \\
&= \frac{1 + \bar{\Gamma}_V(z)e^{\pm j2\beta\lambda/4}}{1 - \bar{\Gamma}_V(z)e^{\pm j2\beta\lambda/4}} = \frac{1 + \bar{\Gamma}_V(z \pm \lambda/4)}{1 - \bar{\Gamma}_V(z \pm \lambda/4)} \\
&= \bar{Z}_n\left(z \pm \frac{\lambda}{4}\right)
\end{aligned} \tag{10.37}$$

Thus $\bar{Y}_n$ at a given value of z is equal to $\bar{Z}_n$ at a value of z located $\lambda/4$ from it. On the Smith Chart this corresponds to the point on the con-

stant SWR circle passing through B and diametrically opposite to it, that is, the point D. Thus,

$$\bar{Y}_{n1} = 0.6 + j0.8$$

and

$$\bar{Y}_1 = Y_{01}\bar{Y}_{n1} = \frac{1}{150}(0.6 + j0.8)$$
$$= (0.004 + j0.0053) \text{ mho}$$

In fact, the Smith Chart can be used as an admittance chart instead of as an impedance chart, that is, by knowing the line admittance at one point on the line, the line admittance at another point on the line can be found by proceeding in the same manner as for impedances. As an example, to find $\bar{Y}_1$, we can first find the normalized line admittance at $z = 0$ by locating the point C diametrically opposite to point A on the constant SWR cirlce. Then we find $\bar{Y}_{n1}$ by simply going on the constant SWR circle by the distance l $(= 0.375\lambda_1)$ toward the generator. This leads to point D, thereby giving us the same result for $\bar{Y}_1$ as found above.

4. SWR on line 1 to the left of jB: To find this, we first locate the normalized line admittance just to the left of jB, which then determines the constant SWR circle corresponding to the portion of line 1 to the left of jB. Thus, noting that $\bar{Y}_2 = \bar{Y}_1 + jB$, or $\bar{Y}_{n2} = \bar{Y}_{n1} + jB/Y_{01}$, and hence

$$\text{Re}[\bar{Y}_{n2}] = \text{Re}[\bar{Y}_{n1}] \tag{10.38a}$$

$$\text{Im}[\bar{Y}_{n2}] = \text{Im}[\bar{Y}_{n1}] + \frac{B}{Y_{01}} \tag{10.38b}$$

we start at point D and go along the constant real part (conductance) circle to reach point E for which the imaginary part differs from the imaginary part at D by the amount B/Y_{01}, that is, $-0.003\Big/\frac{1}{150}$, or -0.45. We then draw the constant SWR circle passing through E and then read off the required SWR value at point F. This value is equal to 1.94.

The steps outlined above in part 4 can be applied in reverse to determine the location and the value of the susceptance required to achieve an SWR of unity to the left of it, that is, a condition of no standing waves. This procedure is known as transmission-line "matching." It is important from the point of view of eliminating or minimizing certain undesirable effects of standing waves in electromagnetic energy transmission.

To illustrate the solution to the matching problem, we first recognize that an SWR of unity is represented by the center point of the Smith Chart. Hence

matching is achieved if $\bar{Y}_{n2}$ falls at the center of the Smith Chart. Now since the difference between $\bar{Y}_{n1}$ and $\bar{Y}_{n2}$ is only in the imaginary part as indicated by (10.38a) and (10.38b), $\bar{Y}_{n1}$ must lie on the constant conductance circle passing through the center of the Smith Chart (this circle is known as the "unit conductance circle" since it corresponds to normalized real part equal to unity). $\bar{Y}_{n1}$ must also lie on the constant SWR circle corresponding to the portion of the line to the right of jB. Hence it is given by the point(s) of intersection of this constant SWR circle and the unit conductance circle. There are two such points G and H, as shown in Fig. 10.10, in which the points A and

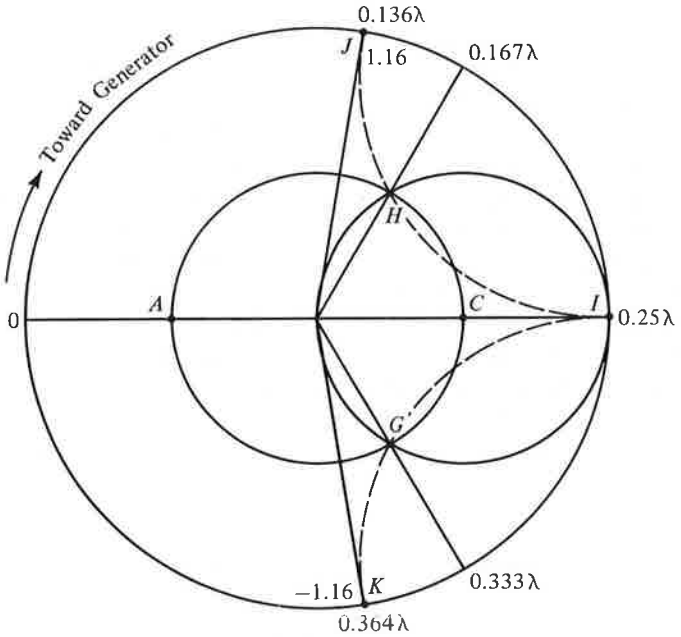

Figure 10.10. Solution of transmission-line matching problem by using the Smith Chart.

C are repeated from Fig. 10.9. There are thus two solutions to the matching problem. If we choose G to correspond to $\bar{Y}_{n1}$, then since the distance from C to G is $(0.333 - 0.250)\lambda_1$, or $0.083\lambda_1$, jB must be located at $z = -0.083\lambda_1$. To find the value of jB, we note that the normalized susceptance value corresponding to G is -1.16 and hence $B/Y_{01} = 1.16$, or $jB = j1.16Y_{01} = j0.00773$ mho. If, however, we choose the point H to correspond to $\bar{Y}_{n1}$, then we find in a similar manner that jB must be located at $z = (0.250 + 0.167)\lambda_1$ or $0.417\lambda_1$ and its value must be $-j0.00773$ mho.

The reactive element jB used to achieve the matching is commonly realized by means of a short-circuited section of line, known as a "stub." This is based on the fact that the input impedance of a short-circuited line is purely

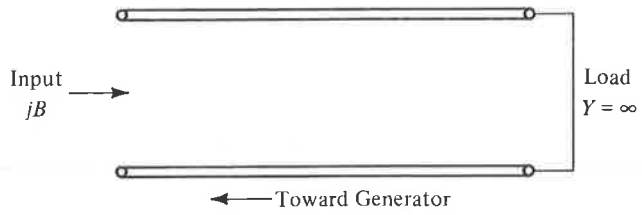

Figure 10.11. A short-circuited stub.

reactive, as shown in Sec. 6.4. The length of the stub for a required input susceptance can be found by considering the short circuit as the load, as shown in Fig. 10.11, and using the Smith Chart. The admittance corresponding to a short circuit is infinity and hence the load admittance normalized with respect to the characteristic admittance of the stub is also equal to infinity. This is located on the Smith Chart at point I in Fig. 10.10. We then go along the constant SWR circle passing through I (the outermost circle) toward the generator (input) until we reach the point corresponding to the required input susceptance of the stub normalized with respect to the characteristic admittance of the stub. Assuming the characteristic impedance of the stub to be the same as that of the line, this quantity is here equal to $j1.16$ or $-j1.16$, depending on whether point G or point H is chosen for the location of the stub. This leads us to point J or point K, and hence the stub length is $(0.25 + 0.136)\lambda_1$, or $0.386\lambda_1$, for $jB = j1.16$, and $(0.364 - 0.25)\lambda_1$, or $0.114\lambda_1$, for $jB = -j1.16$. The arrangement of the stub corresponding to the solution for which the stub location is at $z = -0.083\lambda_1$, and the stub length is $0.386\lambda_1$, is shown in Fig. 10.12.

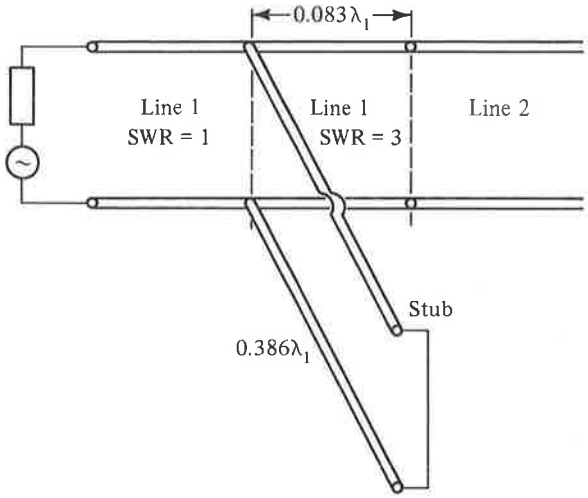

Figure 10.12. A solution to the matching problem for the transmission-line system of Fig. 10.5.

In this section we introduced the Smith Chart, which is a graphical aid in the solution of transmission-line problems. After first discussing the basis behind the construction of the Smith Chart, we illustrated its use by considering a transmission-line system and computing several quantities of interest. We concluded the section with the solution of a transmission-line matching problem.

REVIEW QUESTIONS

10.12. Define line impedance. What is its value for an infinitely long line?

10.13. What is the basis behind the construction of the Smith Chart? How does the Smith Chart simplify the solution of transmission-line problems?

10.14. Briefly discuss the mapping of the normalized line impedances from the complex $\bar{Z}_n$ plane onto the Smith Chart.

10.15. Why is a circle with its center at the center of the Smith Chart known as a constant SWR circle? Where on the circle is the corresponding SWR value marked?

10.16. Using the Smith Chart, how do you find the normalized line admittance at a point on the line given the normalized line impedance at that point?

10.17. Briefly discuss the solution of the transmission-line matching problem.

10.18. How is the length of a short-circuited stub for a required input susceptance determined by using the Smith Chart?

PROBLEMS

10.9. With the aid of a computer program, compute values of $\bar{\Gamma}_V$ corresponding to several points along line a in Fig. 10.6(a) and show that the contour a' in Fig. 10.6(b) is a circle of radius $\frac{1}{2}$ and centered at (1/2, 0).

10.10. With the aid of a computer program, compute values of $\bar{\Gamma}_V$ corresponding to several points along line b in Fig. 10.6(a) and show that the contour b' in Fig. 10.6(b) is a portion of a circle of radius 2 and centered at (1, 2).

10.11. For the transmission-line system of Fig. 10.8, and for the values of Z_{01}, Z_{02}, and l specified in the text, find the value of B which minimizes the SWR to the left of jB. What is the minimum value of SWR?

10.12. In Fig. 10.8 assume $Z_{01} = 300$ ohms, $Z_{02} = 75$ ohms, $B = 0.002$ mho, and $l = 0.145\lambda_1$, and find (a) $\bar{Z}_1$, (b) SWR on line 1 to the right of jB, (c) $\bar{Y}_1$, and (d) SWR on line 1 to the left of jB.

10.13. A transmission line of characteristic impedance 50 ohms is terminated by a load impedance of $(73 + j0)$ ohms. Find the location and the length of a short-circuited stub of characteristic impedance 50 ohms for achieving a match between the line and the load.

10.4 REFLECTION AND REFRACTION OF PLANE WAVES

In Sec. 7.6 we considered oblique incidence of uniform plane waves upon an interface between two dielectric media and found the relationships between the angles of incidence, reflection, and transmission. In this section we shall consider the problem in more detail and derive the expressions for the reflection and transmission coefficients at the boundary. To do this, we distinguish between two cases: (a) the electric field vector of the wave linearly polarized parallel to the interface and (b) the magnetic field vector of the wave linearly polarized parallel to the interface. The law of reflection and Snell's law derived in Sec. 7.6 hold for both cases since they result from the fact that the apparent phase velocities of the incident, reflected, and transmitted waves parallel to the boundary must be equal.

The geometry pertinent to the case of the electric field vector parallel to the interface is shown in Fig. 10.13 in which the interface is assumed to be in the $x = 0$ plane, and the subscripts i, r, and t associated with the field symbols denote incident, reflected, and transmitted waves, respectively. The plane of incidence, that is, the plane containing the normal to the interface and the propagation vectors, is assumed to be in the xz plane so that the electric field vectors are entirely in the y direction. The corresponding magnetic field vectors are then as shown in the figure so as to be consistent with the

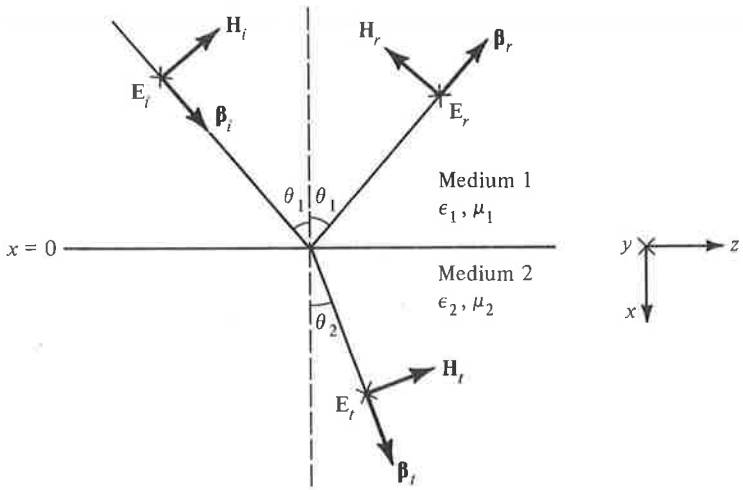

Figure 10.13. For obtaining the reflection and transmission coefficients for an obliquely incident uniform plane wave on a dielectric interface with its electric field perpendicular to the plane of incidence.

condition that **E**, **H**, and **β** form a right-handed mutually orthogonal set of vectors. Since the electric field vectors are perpendicular to the plane of incidence, this case is also said to correspond to perpendicular polarization. The angle of incidence is assumed to be θ_1. From the law of reflection (7.69a), the angle of reflection is then also θ_1. The angle of transmission, assumed to be θ_2, is related to θ_1 by Snell's law, given by (7.69b).

The boundary conditions to be satisfied at the interface $x = 0$ are that (a) the tangential component of the electric field intensity be continuous and (b) the tangential component of the magnetic field intensity be continuous. Thus, we have at the interface $x = 0$

$$E_{yi} + E_{yr} = E_{yt} \tag{10.39a}$$

$$H_{zi} + H_{zr} = H_{zt} \tag{10.39b}$$

Expressing the quantities in (10.39a) and (10.39b) in terms of the total fields, we obtain

$$E_i + E_r = E_t \tag{10.40a}$$

$$H_i \cos\theta_1 - H_r \cos\theta_1 = H_t \cos\theta_2 \tag{10.40b}$$

We also know from one of the properties of uniform plane waves that

$$\frac{E_t}{H_i} = \frac{E_r}{H_r} = \eta_1 = \sqrt{\frac{\mu_1}{\epsilon_1}} \tag{10.41a}$$

$$\frac{E_t}{H_t} = \eta_2 = \sqrt{\frac{\mu_2}{\epsilon_2}} \tag{10.41b}$$

Substituting (10.41a) and (10.41b) into (10.40b) and rearranging, we get

$$E_i - E_r = E_t \frac{\eta_1}{\eta_2} \frac{\cos\theta_2}{\cos\theta_i} \tag{10.42}$$

Solving (10.40a) and (10.42) for E_i and E_r, we have

$$E_i = \frac{E_t}{2}\left(1 + \frac{\eta_1}{\eta_2}\frac{\cos\theta_2}{\cos\theta_1}\right) \tag{10.43a}$$

$$E_r = \frac{E_t}{2}\left(1 - \frac{\eta_1}{\eta_2}\frac{\cos\theta_2}{\cos\theta_1}\right) \tag{10.43b}$$

We now define the reflection coefficient $\Gamma_\perp$ and the transmission coefficient $\tau_\perp$ as

$$\Gamma_\perp = \frac{E_{yr}}{E_{yi}} = \frac{E_r}{E_i} \tag{10.44a}$$

$$\tau_\perp = \frac{E_{yt}}{E_{yi}} = \frac{E_t}{E_i} \tag{10.44b}$$

where the subscript $\perp$ refers to perpendicular polarization. From (10.43a) and (10.43b), we then obtain

$$\Gamma_\perp = \frac{\eta_2 \cos\theta_1 - \eta_1 \cos\theta_2}{\eta_2 \cos\theta_1 + \eta_1 \cos\theta_2} \tag{10.45a}$$

$$\tau_\perp = \frac{2\eta_2 \cos\theta_1}{\eta_2 \cos\theta_1 + \eta_1 \cos\theta_2} \tag{10.45b}$$

Before we discuss the result given by (10.45a) and (10.45b), we shall derive the corresponding expressions for the case in which the magnetic field of the wave is parallel to the interface. The geometry pertinent to this case is shown in Fig. 10.14. Here again the plane of incidence is chosen to be the xz plane so that the magnetic field vectors are entirely in the y direction. The corresponding electric field vectors are then as shown in the figure so as to be consistent with the condition that **E**, **H**, and **β** form a right-handed mutually orthogonal set of vectors. Since the electric field vectors are parallel to the plane of incidence, this case is also said to correspond to parallel polarization.

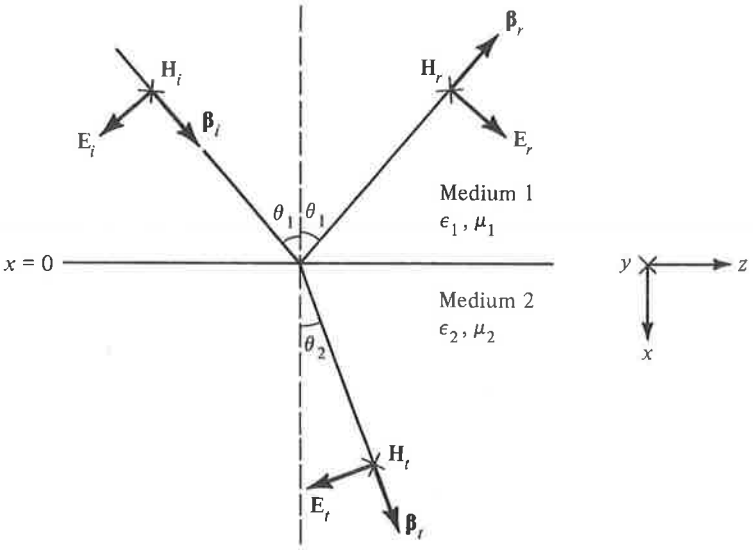

Figure 10.14. For obtaining the reflection and transmission coefficients for an obliquely incident uniform plane wave on a dielectric interface with its electric field parallel to the plane of incidence.

Once again the boundary conditions to be satisfied at the interface $x = 0$ are that (a) the tangential component of the electric field intensity be continous and (b) the tangential component of the magnetic field intensity be continuous. Thus we have at the interface $x = 0$,

$$E_{zi} + E_{zr} = E_{zt} \tag{10.46a}$$

$$H_{yi} + H_{yr} = H_{yt} \tag{10.46b}$$

Expressing the quantities in (10.46a) and (10.46b) in terms of the total fields and also using (10.41a) and (10.41b), we obtain

$$E_i - E_r = E_t \frac{\cos \theta_2}{\cos \theta_1} \tag{10.47a}$$

$$E_i + E_r = E_t \frac{\eta_1}{\eta_2} \tag{10.47b}$$

Solving (10.47a) and (10.47b) for E_i and E_r, we have

$$E_i = \frac{E_t}{2}\left(\frac{\eta_1}{\eta_2} + \frac{\cos \theta_2}{\cos \theta_1}\right) \tag{10.48a}$$

$$E_r = \frac{E_t}{2}\left(\frac{\eta_1}{\eta_2} - \frac{\cos \theta_2}{\cos \theta_1}\right) \tag{10.48b}$$

We now define the reflection coefficient $\Gamma_{||}$ and the transmission coefficient $\tau_{||}$ as

$$\Gamma_{||} = \frac{E_{zr}}{E_{zi}} = \frac{E_r \cos \theta_1}{-E_i \cos \theta_1} = -\frac{E_r}{E_i} \tag{10.49a}$$

$$\tau_{||} = \frac{E_{zt}}{E_{zi}} = \frac{-E_t \cos \theta_2}{-E_i \cos \theta_1} = \frac{E_t}{E_i}\frac{\cos \theta_2}{\cos \theta_1} \tag{10.49b}$$

where the subscript || refers to parallel polarization. From (10.48a) and (10.48b), we then obtain

$$\Gamma_{||} = \frac{\eta_2 \cos \theta_2 - \eta_1 \cos \theta_1}{\eta_2 \cos \theta_2 + \eta_1 \cos \theta_1} \tag{10.50a}$$

$$\tau_{||} = \frac{2\eta_2 \cos \theta_2}{\eta_2 \cos \theta_2 + \eta_1 \cos \theta_1} \tag{10.50b}$$

We shall now discuss the results given by (10.45a), (10.45b), (10.50a), and (10.50b) for the reflection and transmission coefficients for the two cases:

1. For $\theta_1 = 0$, that is, for the case of normal incidence of the uniform plane wave upon the interface, $\theta_2 = 0$ and

$$\Gamma_\perp = \frac{\eta_2 - \eta_1}{\eta_2 + \eta_1}, \qquad \Gamma_{||} = \frac{\eta_2 - \eta_1}{\eta_2 + \eta_1}$$

$$\tau_\perp = \frac{2\eta_2}{\eta_2 + \eta_1}, \qquad \tau_{||} = \frac{2\eta_2}{\eta_2 + \eta_1}$$

Thus the reflection coefficients as well as the transmission coefficients for the two cases become equal as they should since for normal incidence, there is no difference between the two polarizations except for rotation by 90° parallel to the interface.

2. $\Gamma_\perp = 1$ and $\Gamma_{||} = -1$ if $\cos\theta_2 = 0$, that is,

$$\sqrt{1 - \sin^2\theta_2} = \sqrt{1 - \frac{\mu_1\epsilon_1}{\mu_2\epsilon_2}\sin^2\theta_1} = 0$$

or

$$\sin\theta_1 = \sqrt{\frac{\mu_2\epsilon_2}{\mu_1\epsilon_1}} \tag{10.51}$$

where we have used Snell's law given by (7.69b) to express $\sin\theta_2$ in terms of $\sin\theta_1$. If we assume $\mu_2 = \mu_1 = \mu_0$ as is usually the case, (10.51) has real solutions for θ_1 for $\epsilon_2 < \epsilon_1$. Thus, for $\epsilon_2 < \epsilon_1$, that is, for transmission from a dielectric medium of higher permittivity into a dielectric medium of lower permittivity, there is a critical angle of incidence θ_c given by

$$\theta_c = \sin^{-1}\sqrt{\frac{\epsilon_2}{\epsilon_1}} \tag{10.52}$$

for which θ_2 is equal to 90°, and $|\Gamma_\perp| = |\Gamma_{||}| = 1$. For $\theta_1 > \theta_c$, $\sin\theta_2$ becomes greater than 1, $\cos\theta_2$ becomes imaginary, and $|\Gamma_\perp| = |\Gamma_{||}| = 1$. This is consistent with the phenomenon of "total internal reflection" for $\theta_1 > \theta_c$, which we discussed in Sec. 7.6.

3. $\Gamma_\perp = 0$ for $\eta_2\cos\theta_1 = \eta_1\cos\theta_2$, that is

$$\eta_2\sqrt{1 - \sin^2\theta_1} = \eta_1\sqrt{1 - \frac{\mu_1\epsilon_1}{\mu_2\epsilon_2}\sin^2\theta_1}$$

or

$$\sin^2\theta_1 = \frac{\eta_2^2 - \eta_1^2}{\eta_2^2 - \eta_1^2(\mu_1\epsilon_1/\mu_2\epsilon_2)} = \mu_2\frac{\mu_2 - \mu_1(\epsilon_2/\epsilon_1)}{\mu_2^2 - \mu_1^2} \tag{10.53}$$

For the usual case of transmission between two dielectric materials, that is, for $\mu_2 = \mu_1$, and $\epsilon_2 \neq \epsilon_1$, this equation has no real solution for θ_1 and hence there is no angle of incidence for which the reflection coefficient is zero for the case of perpendicular polarization.

4. $\Gamma_{||} = 0$ for $\eta_2\cos\theta_2 = \eta_1\cos\theta_1$, that is,

$$\eta_2\sqrt{1 - \frac{\mu_1\epsilon_1}{\mu_2\epsilon_2}\sin^2\theta_1} = \eta_1\sqrt{1 - \sin^2\theta_1}$$

or

$$\sin^2\theta_1 = \frac{\eta_2^2 - \eta_1^2}{\eta_2^2(\mu_1\epsilon_1/\mu_2\epsilon_2) - \eta_1^2} = \epsilon_2\frac{(\mu_2/\mu_1)\epsilon_1 - \epsilon_2}{\epsilon_1^2 - \epsilon_2^2} \tag{10.54}$$

If we assume $\mu_2 = \mu_1$, this equation reduces to

$$\sin^2\theta_1 = \frac{\epsilon_2}{\epsilon_1 + \epsilon_2}$$

which then gives

$$\cos^2\theta_1 = 1 - \sin^2\theta_1 = \frac{\epsilon_1}{\epsilon_1 + \epsilon_2}$$

and

$$\tan\theta_1 = \sqrt{\frac{\epsilon_2}{\epsilon_1}}$$

Thus there exists a value of the angle of incidence θ_p, given by

$$\theta_p = \tan^{-1}\sqrt{\frac{\epsilon_2}{\epsilon_1}} \tag{10.55}$$

for which the reflection coefficient is zero and hence there is complete transmission for the case of parallel polarization.

5. In view of (3) and (4) above, for an elliptically polarized wave incident on the interface at the angle θ_p, the reflected wave will be linearly polarized perpendicular to the plane of incidence. For this reason, the angle θ_p is known as the "polarizing angle." It is also known as the "Brewster angle." The phenomenon associated with the Brewster angle has several applications. An example is in gas lasers in which the discharge tube lying between the mirrors of a Fabry Perot resonator is sealed by glass windows placed at the Brewster angle, as shown in Fig. 10.15, to minimize reflections from the ends of the tube so that the laser behavior is governed by the mirrors external to the tube.

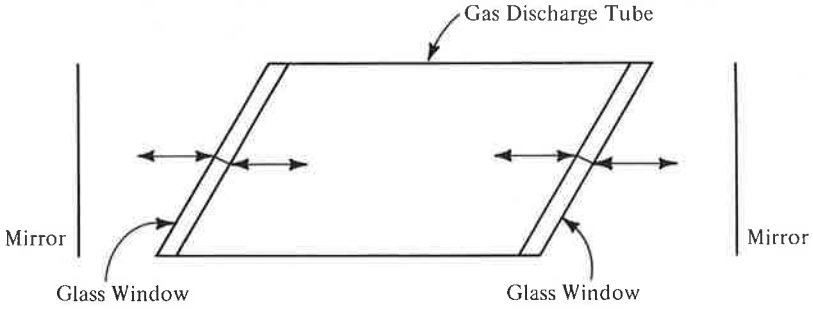

Figure 10.15. For illustrating the application of the Brewster angle effect in gas lasers.

In this section we considered oblique incidence of a uniform plane wave upon the boundary between two perfect dielectric media and derived the expressions for the reflection and transmission coefficients for the cases of perpendicular and parallel polarizations. An examination of these expressions revealed that (a) for incidence from a dielectric medium of higher permittivity onto one of lower permittivity, there is a critical angle of incidence beyond which total internal reflection occurs, as we learned in Sec. 7.6, and (b) for the case of parallel polarization, there is an angle of incidence, known as the Brewster angle, for which the reflection coefficient is zero.

REVIEW QUESTIONS

10.19. What is meant by the plane of incidence? Distinguish between the two different linear polarizations pertinent to the derivation of the reflection and transmission coefficients for oblique incidence on a dielectric interface.

10.20. Briefly discuss the determination of the reflection and transmission coefficients for an obliquely incident wave on a dielectric interface.

10.21. What is the nature of the reflection coefficient for angle of incidence greater than the critical angle for total internal reflection?

10.22. What is the Brewester angle? What is the polarization of the reflected wave for an elliptically polarized wave incident on a dielectric interface at the Brewster angle?

10.23. Discuss an application of the Brewster angle effect.

PROBLEMS

10.14. A uniform plane wave having the electric field given by

$$\mathbf{E} = E_0 \mathbf{i}_y \sin [6\pi \times 10^9 t - 10\pi(x + \sqrt{3}\, z)]$$

is incident on the interface between free space and a dielectric of permittivity $1.5\epsilon_0$ as shown in Fig. 10.16. (a) Obtain the expression for the reflected wave field. (b) Obtain the expression for the transmitted wave field.

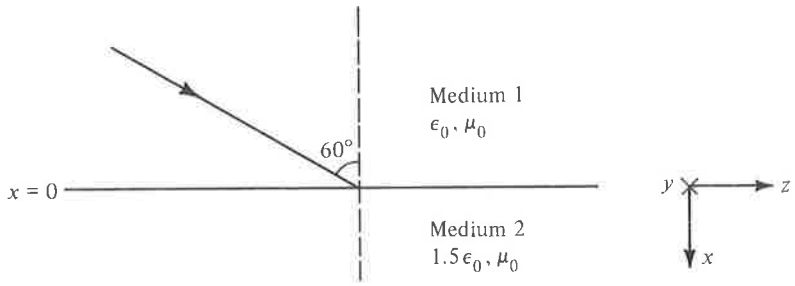

Figure 10.16. For Problem 10.14.

10.15. Repeat Problem 10.14 for the uniform plane wave having the electric field given by

$$\mathbf{E} = E_0\left(\frac{\sqrt{3}}{2}\mathbf{i}_x - \frac{1}{2}\mathbf{i}_z\right)\cos\left[6\pi \times 10^9 t - 10\pi(x + \sqrt{3}\,z)\right]$$

10.16. Repeat Problem 10.14 for the uniform plane wave having the electric field given by

$$\mathbf{E} = E_0\left(\frac{\sqrt{3}}{2}\mathbf{i}_x - \frac{1}{2}\mathbf{i}_z\right)\cos\left[6\pi \times 10^9 t - 10\pi(x + \sqrt{3}\,z)\right]$$
$$+ E_0\mathbf{i}_y \sin\left[6\pi \times 10^9 t - 10\pi(x + \sqrt{3}\,z)\right]$$

Also discuss the polarizations of the incident, reflected, and transmitted waves.

10.17. For the dielectric boundary in Fig. 10.16, determine the angle of incidence of an elliptically polarized wave for the reflected wave to be linearly polarized. In which plane is the reflected wave polarized then?

10.5 DESIGN OF A FREQUENCY-INDEPENDENT ANTENNA

In Chap. 8 we studied the directional properties of antennas and antenna arrays. These properties depend on the electrical dimensions of the antenna, that is, the dimensions expressed in terms of the wavelength at the operating frequency. Hence an antenna of fixed physical dimensions exhibits frequency-dependent characteristics. This very fact suggests that for an antenna to be frequency-independent, its electrical size must remain constant with frequency and hence its physical size should increase proportionately to the wavelength. Alternatively, for an antenna of fixed physical dimensions, the active region, that is, the region responsible for the predominant radiation should vary with frequency, that is, scale itself in such a manner that its electrical size remains the same.

A simple illustration of the aforementioned property is provided by the equiangular spiral antenna shown in Fig. 10.17 and so-termed because the angle between the radius vector from the origin and the spiral remains the same for all points on the curve. The equiangular spiral antenna was proposed by Rumsey in 1954 during the early stages of research on frequency-independent antennas at the University of Illinois. When this antenna is excited at the origin, the current flows outward with small attenuation along the spiral until an active region is reached from which essentially all of the incident energy transmitted along the spiral arms is radiated. Since this active region is of constant size in wavelengths, it moves toward the origin as the operating wavelength decreases or the frequency increases. The size of the effective radiating region thus adjusts automatically with the operating frequency such that the antenna behaves the same at all frequencies except for

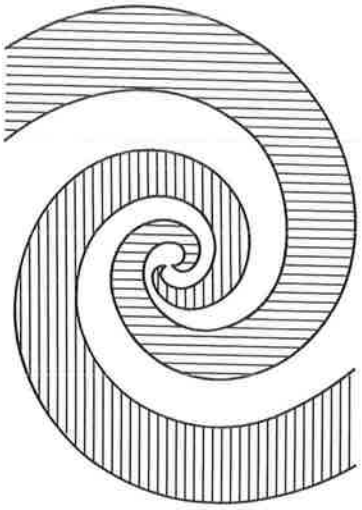

Figure 10.17. The equiangular spiral antenna.

a rotation of the radiated field about the antenna axis because of the spiraling of the arms.

Another and more conventional example of a frequency-independent antenna is the "log-periodic dipole array," shown in Fig. 10.18. As the name implies, it employs a number of dipoles. The dipole lengths and the spacings between consecutive dipoles increase along the array by a constant scale factor such that

$$\frac{l_{i+1}}{l_i} = \frac{d_{i+1}}{d_i} = \tau \tag{10.56}$$

From the principle of scaling, it is evident that for this structure extending from zero to infinity and energized at the apex, the properties repeat at frequencies given by $\tau^n f$, where n takes integer values. When plotted on a logarithmic scale, these frequencies are equally spaced at intervals of $\log \tau$. It is for this reason that the structure is termed "log-periodic."

The log-periodic dipole array is fed by a transmission line, as shown in Fig. 10.18, such that a 180°-phase shift is introduced between successive elements in addition to that corresponding to the spacing between the elements. The resulting radiation pattern is directed toward the apex, that is toward the source. Almost all of the radiation takes place from those elements which are in the vicinity of a half wavelength long. The operating band of frequencies is therefore bounded on the low side by frequencies at which the largest elements are approximately a half wavelength long and on the high side by frequencies corresponding to the size of the smallest elements. As the frequency is varied, the radiating or active region moves back and forth along

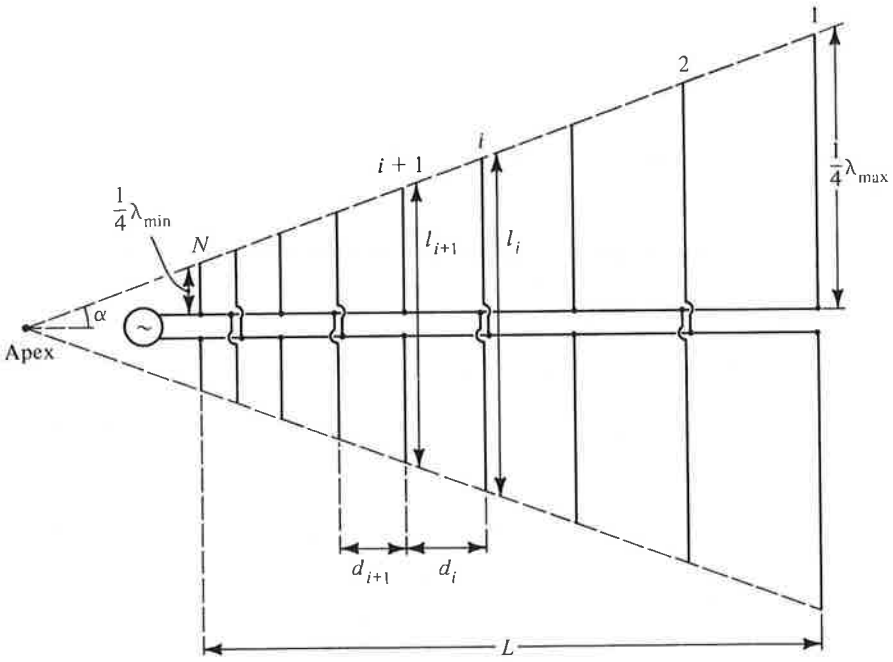

Figure 10.18. Log-periodic dipole array.

the array. Since practically all of the input power is radiated by the active region, the larger elements to the right of it are not excited. Furthermore, because the radiation is toward the apex, these larger elements are essentially in a field-free region and hence do not significantly influence the operation. Although the shorter elements to the left of the active region are in the antenna beam, they have small influence on the pattern because of their short lengths, close spacings, and the 180°-phase shift.

We shall now discuss the design of a log-periodic dipole array. We shall restrict the design to the computation of the lengths and spacings of the elements for a specified bandwidth of operation and directivity of the radiation pattern. The design parameters are the scale factor τ given by (10.56), the half angle α subtended at the apex, and the ratio σ of the element spacing to twice the length of the next larger element. Since the active region is not of negligible length along the structure, the array is designed for a larger bandwidth than the design specification. This larger bandwidth is known as the "bandwidth of the structure," denoted B_s. The ratio of B_s to the design bandwidth B is termed the "bandwidth of the active region," B_{ar} and is related to σ and τ.* We shall first present the relevant definitions and formulas, with

*The relationship between B_{ar}, σ and τ and other design curves have been obtained by R. L. Carrell in a Ph.D. dissertation at the University of Illinois.

reference to Fig. 10.18:

$$\tau = \frac{d_{i+1}}{d_i} = \frac{l_{i+1}}{l_i} = \text{scale factor}$$

$$\sigma = \frac{d_i}{2l_i} = \text{relative spacing constant}$$

α = half apex angle

L = boom length, that is, the distance between the shortest and longest element

N = number of elements

B_s = bandwidth of the structure

$$= \frac{\lambda_{\max}}{\lambda_{\min}} = B_{ar}B \tag{10.57}$$

B_{ar} = bandwidth of the active region

$$= 1.1 + 7.7(1 - \tau)^2 \cot \alpha \tag{10.58}$$

Since

$$\tan \alpha = \frac{l_i - l_{i+1}}{2d_i} = \frac{1 - \tau}{4\sigma}$$

we obtain

$$\alpha = \tan^{-1} \frac{1 - \tau}{4\sigma} \tag{10.59}$$

From

$$\cot \alpha = \frac{L}{(\lambda_{\max}/4) - (\lambda_{\min}/4)}$$

we have

$$L = \left[\frac{1}{4}\left(1 - \frac{1}{B_s}\right) \cot \alpha\right] \lambda_{\max} \tag{10.60}$$

From

$$\frac{\lambda_{\min}}{\lambda_{\max}} = \frac{l_N}{l_1} = \tau^{N-1}$$

we obtain

$$B_s = \left(\frac{1}{\tau}\right)^{N-1}$$

$$\log B_s = (N - 1) \log \frac{1}{\tau}$$

$$N = 1 + \frac{\log B_s}{\log (1/\tau)} \tag{10.61}$$

Let us now consider an example in which it is desired to design a log-periodic dipole array for which the band of operation is from 12.5 MHz to 30 MHz and the directivity is 9. In terms of decibels, the directivity is $20 \log_{10} 3$, or 9.5 db. The design consists of the following steps:

1. Compute the design bandwidth B.

$$B = \frac{30}{12.5} = 2.4$$

2. Find τ and σ to give the desired directivity. There exists an optimum σ for which the directivity is maximum for each value of τ in the range $0.8 < \tau < 1.0$. Plots of this optimum σ and the corresponding τ versus the directivity are shown in Fig. 10.19. For the desired directivity of 9.5 db, we have from Fig. 10.19,

$$\tau = 0.893$$
$$\sigma = 0.163$$

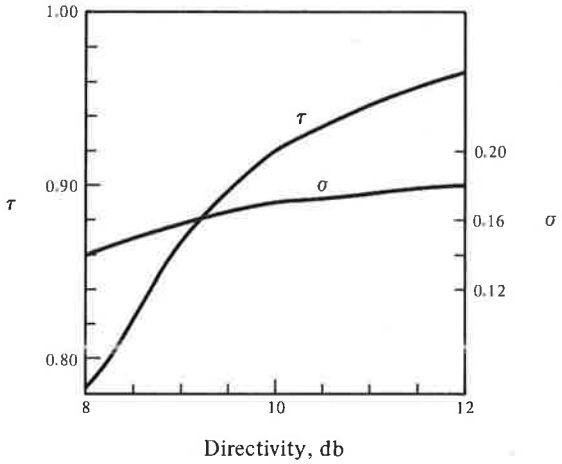

Figure 10.19. Plots of optimum σ and the corresponding τ versus directivity for log-periodic dipole arrays.

3. Determine the half apex angle α from (10.59).

$$\alpha = \tan^{-1} \frac{1 - 0.893}{4 \times 0.163} = 9.32°$$

4. Determine the bandwidth of the active region B_{ar} from (10.58).

$$B_{ar} = 1.1 + 7.7(1 - 0.893)^2 \cot 9.32° = 1.637$$

5. Determine the bandwidth of the structure B_s from (10.57).

$$B_s = 1.637 \times 2.4 = 3.929$$

6. Determine the boom length L from (10.60). Assuming the longest element to be a half wavelength long at the low frequency end of the specified band, $\lambda_{max} = 24$ m and,

$$L = \left[\frac{1}{4}\left(1 - \frac{1}{3.929}\right)\cot 9.32^\circ\right]24 = 27.25 \text{ m}$$

7. Determine the number of elements N from (10.61).

$$N = 1 + \frac{\log 3.929}{\log (1/0.893)} = 13$$

8. Determine the element lengths and spacings:

$$l_1 = \frac{\lambda_{max}}{2} = \frac{24}{2} = 12 \text{ m}$$
$$l_2 = l_1\tau = 12 \times 0.893 = 10.72 \text{ m}$$
$$l_3 = l_2\tau = 10.72 \times 0.893 = 9.57 \text{ m}$$
$$\cdots$$
$$d_1 = \frac{l_1 - l_2}{2}\cot\alpha = 0.64 \cot 9.32^\circ = 3.91 \text{ m}$$
$$d_2 = d_1\tau = 3.91 \times 0.893 = 3.49 \text{ m}$$
$$d_3 = d_2\tau = 3.49 \times 0.893 = 3.12 \text{ m}$$
$$\cdots$$

Values of the element lengths and spacings and the nearest frequencies at which the elements are a half wavelength long are listed in Table 10.1.

In this section we introduced the concept of frequency-independent antennas based upon the criterion that for the antenna characteristics to be frequency-independent, the active region must vary with frequency such that its electrical size remains approximately constant. We discussed in particular the log-periodic dipole antenna array and illustrated by means of a numerical example the computation of element lengths and spacings for desired operating bandwidth and directivity.

TABLE 10.1. Computed Values of Log-Periodic Dipole Array Element Parameters

Element number	*Length* (m)	*Spacing* (m)	*Frequency* (MHz)
1	12.00	—	12.50
2	10.72	3.91	14.00
3	9.57	3.49	15.67
4	8.55	3.12	17.55
5	7.63	2.78	19.66
6	6.81	2.49	22.01
7	6.09	2.22	24.65
8	5.43	1.98	27.60
9	4.85	1.77	30.91
10	4.33	1.58	34.61
11	3.87	1.41	38.76
12	3.46	1.26	43.41
13	3.09	1.13	48.61

REVIEW QUESTIONS

10.24. Discuss the criterion for an antenna of fixed physical size to be frequency-independent.

10.25. Describe how the equiangular spiral antenna has frequency-independent characteristics.

10.26. What is a log-periodic dipole array? Briefly discuss its operation.

10.27. Why is a log-periodic dipole array designed for a larger bandwidth than the design specification?

10.28. Outline the steps in the design of a log-periodic dipole array.

PROBLEMS

10.18. Design a log-periodic dipole array for operation over the frequency band from 54 MHz to 108 MHz (VHF TV channels 2 to 6 and FM band) and a directivity of 10 db.

10.19. A log-periodic dipole array is to cover the frequency band from 50 MHz to 250 MHz. Find the boom length and the number of elements for directivity of (a) 9.5 db and (b) 12 db.

10.6 CAPACITANCE OF A PARALLEL-WIRE LINE

In Sec. 9.3 we illustrated the solution of Laplace's equation for the parallel-plate case and discussed the applicability of the static field technique

in the determination of transmission-line parameters. In this section we shall use the technique to obtain an analytical expression for the capacitance of a parallel-wire line, consisting of two infinitely long, straight, parallel, cylindrical wires.

Let us first consider an infinitely long, straight, line charge of uniform density ρ_{L0} C/m situated along the z axis, as shown in Fig. 10.20(a), and obtain the electric potential due to the line charge. The symmetry of the problem indicates that the potential is dependent only on the cylindrical coordinate r. Noting then from Appendix B that in cylindrical coordinates,

$$\nabla^2 V = \nabla \cdot \nabla V = \frac{1}{r}\frac{\partial}{\partial r}\left(r\frac{\partial V}{\partial r}\right)$$

we have from Laplace's equation

$$\frac{1}{r}\frac{\partial}{\partial r}\left(r\frac{\partial V}{\partial r}\right) = 0 \qquad \text{for } r \neq 0 \tag{10.62}$$

Integrating twice, we obtain the solution for (10.62) to be

$$V = A \ln r + B \tag{10.63}$$

where A and B are arbitrary constants. We can arbitrarily set the potential

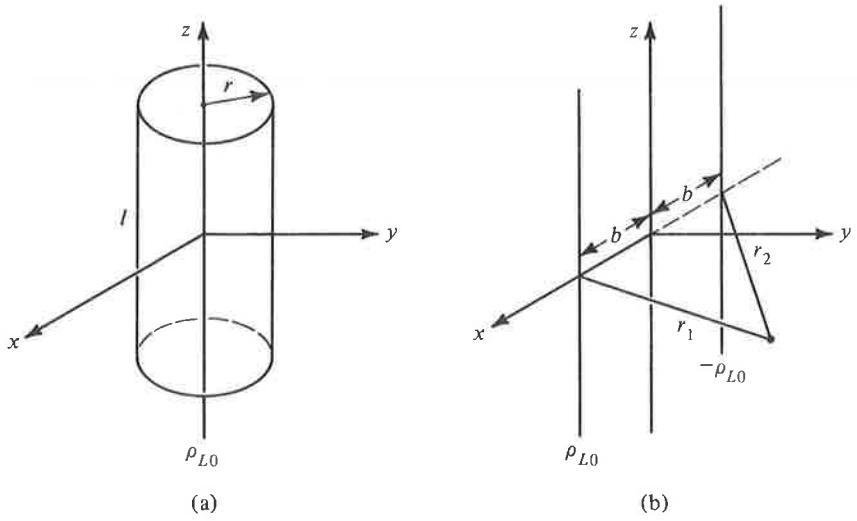

Figure 10.20. (a) An infinitely long line charge of uniform density along the z axis. (b) A pair of parallel, infinitely long line charges of equal and opposite uniform densities.

to be zero at a reference value $r = r_0$ giving us

$$0 = A \ln r_0 + B \qquad \text{or} \qquad B = -A \ln r_0$$

and

$$V = A \ln r - A \ln r_0 = A \ln \frac{r}{r_0} \tag{10.64}$$

To evaluate the arbitrary constant A in (10.64), we find that the electric field intensity due to the line charge is given by

$$\mathbf{E} = -\nabla V = -\frac{\partial V}{\partial r}\mathbf{i}_r = -\frac{A}{r}\mathbf{i}_r$$

The electric field is thus directed radial to the line charge. Let us now consider a cylindrical box of radius r and length l coaxial with the line charge, as shown in Fig. 10.20(a), and apply Gauss' law for the electric field in integral form to the surface of the box. For the cylindrical surface,

$$\int \mathbf{D} \cdot d\mathbf{S} = -\frac{\epsilon A}{r}(2\pi r l)$$

For the top and bottom surfaces, $\int \mathbf{D} \cdot d\mathbf{S} = 0$ since the field is parallel to the surfaces. The charge enclosed by the box is $\rho_{L0} l$. Thus we have

$$-\frac{\epsilon A}{r}(2\pi r l) = \rho_{L0} l \qquad \text{or} \qquad A = -\frac{\rho_{L0}}{2\pi\epsilon}$$

Substituting this result in (10.64) we obtain the potential field due to the line charge to be

$$V = -\frac{\rho_{L0}}{2\pi\epsilon} \ln \frac{r}{r_0} = \frac{\rho_{L0}}{2\pi\epsilon} \ln \frac{r_0}{r} \tag{10.65}$$

Let us now consider two infinitely long, straight, line charges of equal and opposite uniform charge densities ρ_{L0} C/m and $-\rho_{L0}$ C/m, parallel to the z axis and passing through $x = b$ and $x = -b$, respectively, as shown in Fig. 10.20(b). Applying superposition and using (10.65), we write the potential due to the two line charges as

$$V = \frac{\rho_{L0}}{2\pi\epsilon} \ln \frac{r_{01}}{r_1} - \frac{\rho_{L0}}{2\pi\epsilon} \ln \frac{r_{02}}{r_2} \tag{10.66}$$

where r_1 and r_2 are the distances of the point of interest from the line charges and r_{01} and r_{02} are the distances to the reference point at which the potential

is zero. By choosing the reference point to be equidistant from the two line charges, that is, $r_{01} = r_{02}$, we get

$$V = \frac{\rho_{L0}}{2\pi\epsilon} \ln \frac{r_2}{r_1} \tag{10.67}$$

From (10.67), we note that the equipotential surfaces for the potential field of the line-charge pair are given by

$$\frac{r_2}{r_1} = \text{constant, say, } k \tag{10.68}$$

where k lies between 0 and ∞. In terms of Cartesian coordinates, (10.68) can be written as

$$\frac{(x+b)^2 + y^2}{(x-b)^2 + y^2} = k^2 \tag{10.69}$$

Rearranging (10.69), we obtain

$$x^2 - 2b\frac{k^2+1}{k^2-1}x + y^2 + b^2 = 0$$

or

$$\left(x - b\frac{k^2+1}{k^2-1}\right)^2 + y^2 = \left(b\frac{2k}{k^2-1}\right)^2 \tag{10.70}$$

Equation (10.70) represents cylinders having their axes along

$$x = b\frac{k^2+1}{k^2-1}, \qquad y = 0$$

and radii equal to $b\dfrac{2k}{k^2-1}$. The corresponding potentials are $(\rho_{L0}/2\pi\epsilon) \ln k$. The cross sections of the equipotential surfaces are shown in Fig. 10.21.

We can now place perfectly conducting cylinders in any two equipotential surfaces without disturbing the field configuration, as shown, for example, by the thick circles in Fig. 10.21, thereby obtaining a parallel-wire line. Letting the distance between their centers be $2d$ and their radii be a, we have

$$\pm d = b\frac{k^2+1}{k^2-1} \tag{10.71a}$$

$$a = b\frac{2k}{k^2-1} \tag{10.71b}$$

Solving (10.71a) and (10.71b) for k and accepting only those solutions lying between 0 and ∞, we obtain

$$k = \frac{d \pm \sqrt{d^2 - a^2}}{a} \tag{10.72}$$

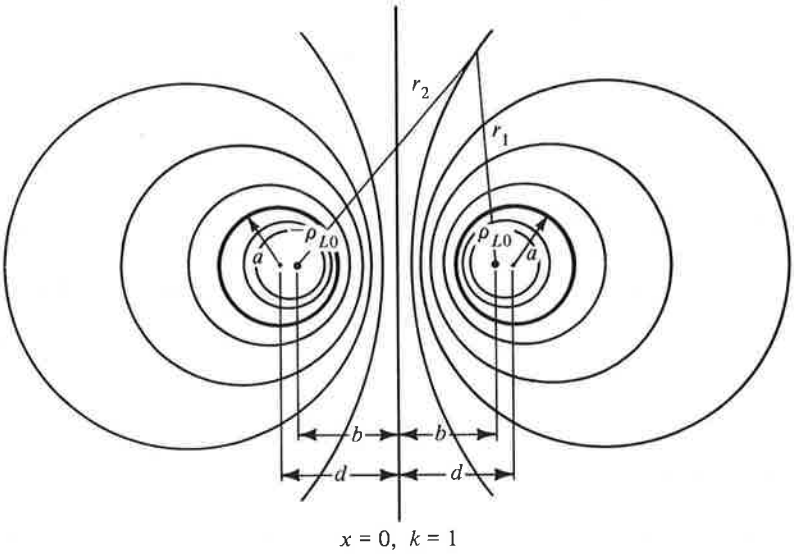

Figure 10.21. Cross sections of equipotential surfaces for the line-charge pair of Fig. 10.20(a). Thick circles represent cross section of parallel-wire line.

The potentials of the right ($k > 1$) and left ($k < 1$) conductors are then given, respectively, by

$$V_+ = \frac{\rho_{L0}}{2\pi\epsilon} \ln \frac{d + \sqrt{d^2 - a^2}}{a} \tag{10.73a}$$

$$V_- = \frac{\rho_{L0}}{2\pi\epsilon} \ln \frac{d - \sqrt{d^2 - a^2}}{a}$$

$$= -\frac{\rho_{L0}}{2\pi\epsilon} \ln \frac{d + \sqrt{d^2 - a^2}}{a} \tag{10.73b}$$

The potential difference between the two conductors is

$$V_0 = V_+ - V_- = \frac{\rho_{L0}}{\pi\epsilon} \ln \frac{d + \sqrt{d^2 - a^2}}{a} \tag{10.74}$$

Finally, to find the capacitance, we note that since the electric field lines begin on the positive charge and end on the negative charge orthogonal to the equipotentials, the magnitude of the charge on either conductor, which produces the same field as the line-charge pair, must be the same as the line charge itself. Thus considering unit length of the line, we obtain the capacitance per unit length of the parallel-wire line to be

$$\mathcal{C} = \frac{\rho_{L0}}{V_0} = \frac{\pi\epsilon}{\ln\left[(d + \sqrt{d^2 - a^2})/a\right]}$$

$$= \frac{\pi\epsilon}{\cosh^{-1}(d/a)} \tag{10.75}$$

In this section we obtained the electric potential field of two parallel, infinitely long, straight, line charges of equal and opposite uniform charge densities and we showed that the equipotential surfaces are cylinders having their axes parallel to the line charges. By placing conductors in two equipotential surfaces, thereby forming a parallel-wire line, we obtained the expression for the capacitance per unit length of the line.

REVIEW QUESTIONS

10.29. Discuss the applicability of static field techniques in the determination of transmission-line parameters.

10.30. Briefly discuss the solution for the potential field of the infinitely long, straight, line charge of uniform density.

10.31. Describe the equipotential surfaces for the potential field of two parallel, infinitely long, straight, line charges of equal and opposite uniform densities. What are the shapes of the direction lines of the electric field?

10.32. Briefly discuss the determination of the capacitance of the parallel-wire line from the potential field of the line-charge pair.

PROBLEMS

10.20. For the line-charge pair of Fig. 10.21, show that the direction lines of the electric field are arcs of circles emanating from the positively charged line and terminating on the negatively charged line.

10.21. For the parallel-wire line, show that for $d \gg a$, the capacitance per unit length of the line is $\frac{\pi\epsilon}{\ln(2d/a)}$. Find the value of d/a for which the exact value of the capacitance per unit length is 1.1 times the value given by the approximate expression for $d \gg a$.

10.22. Figure 10.22 shows the cross-sectional view of an arrangement of two infinitely long, parallel, cylindrical conductors of radii a and b and with their axes separated by distance d. Show that the capacitance per unit length of the arrangement is $2\pi\epsilon/\cosh^{-1}[(a^2 + b^2 - d^2)/2ab]$.

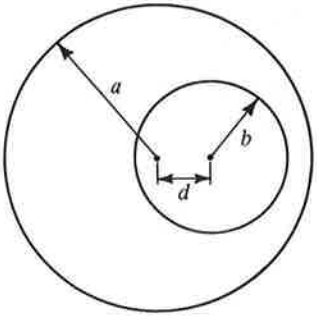

Figure 10.22. For Problem 10.22.

10.7 MAGNETIC VECTOR POTENTIAL

In Sec. 9.1 we learned that since

$$\nabla \times \mathbf{E} = 0$$

for the static electric field, $\mathbf{E}$ can be expressed as the gradient of a scalar potential in the manner

$$\mathbf{E} = -\nabla V$$

We then proceeded with the discussion of the electric scalar potential and its application for the computation of static electric fields. In this section we shall introduce a similar tool for the magnetic field computation, namely, the magnetic vector potential. When extended to the time-varying case, the magnetic vector potential has useful application in the determination of fields due to antennas.

To introduce the magnetic vector potential concept, we recall that the divergence of the magnetic flux density vector, whether static or time-varying, is equal to zero, that is,

$$\nabla \cdot \mathbf{B} = 0 \tag{10.76}$$

If the divergence of a vector is zero, then that vector can be expressed as the curl of another vector since the divergence of the curl of a vector is identically equal to zero, as can be seen by expansion in Cartesian coordinates:

$$\nabla \cdot \nabla \times \mathbf{A} = \left(\mathbf{i}_x \frac{\partial}{\partial x} + \mathbf{i}_y \frac{\partial}{\partial y} + \mathbf{i}_z \frac{\partial}{\partial z}\right) \cdot \begin{vmatrix} \mathbf{i}_x & \mathbf{i}_y & \mathbf{i}_z \\ \frac{\partial}{\partial x} & \frac{\partial}{\partial y} & \frac{\partial}{\partial z} \\ A_x & A_y & A_z \end{vmatrix}$$

$$= \begin{vmatrix} \frac{\partial}{\partial x} & \frac{\partial}{\partial y} & \frac{\partial}{\partial z} \\ \frac{\partial}{\partial x} & \frac{\partial}{\partial y} & \frac{\partial}{\partial z} \\ A_x & A_y & A_z \end{vmatrix} = 0$$

Thus the magnetic field vector **B** can be expressed as the curl of a vector **A**, that is,

$$\mathbf{B} = \nabla \times \mathbf{A} \tag{10.77}$$

The vector **A** is known as the magnetic vector potential in analogy with the electric scalar potential for V.

If we can now find **A** due to an infinitesimal current element, we can then find **A** for a given current distribution and determine **B** by using (10.77). Let us therefore consider an infinitesimal current element of length $d\mathbf{l}$ situated at the origin and oriented along the z axis as shown in Fig. 10.23. Assuming first that the current is constant, say, I amperes, we note from (1.68) that the magnetic field at a point P due to the current element is given by

$$\mathbf{B} = \frac{\mu}{4\pi} \frac{I\, d\mathbf{l} \times \mathbf{i}_r}{r^2} \tag{10.78}$$

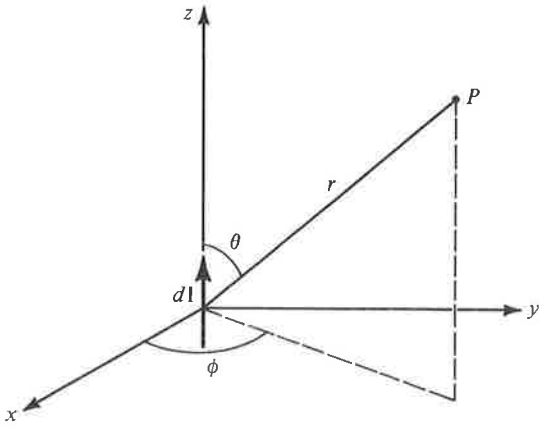

Figure 10.23. For finding the magnetic vector potential due to an infinitesimal current element.

where r is the distance from the current element to the point P and $\mathbf{i}_r$ is the unit vector directed from the element toward P. Expressing $\mathbf{B}$ as

$$\mathbf{B} = \frac{\mu}{4\pi} I\, d\mathbf{l} \times \left(-\nabla \frac{1}{r}\right) \tag{10.79}$$

and using the vector identity

$$\mathbf{A} \times \nabla V = V\nabla \times \mathbf{A} - \nabla \times (V\mathbf{A}) \tag{10.80}$$

we obtain

$$\mathbf{B} = -\frac{\mu I}{4\pi r} \nabla \times d\mathbf{l} + \nabla \times \left(\frac{\mu I\, d\mathbf{l}}{4\pi r}\right) \tag{10.81}$$

Since $d\mathbf{l}$ is a constant, $\nabla \times d\mathbf{l} = 0$, and (10.81) reduces to

$$\mathbf{B} = \nabla \times \left(\frac{\mu I\, d\mathbf{l}}{4\pi r}\right) \tag{10.82}$$

Comparing (10.82) with (10.77), we now see that the vector potential due to the current element situated at the origin is simply given by

$$\mathbf{A} = \frac{\mu I\, d\mathbf{l}}{4\pi r} \tag{10.83}$$

Thus it has a magnitude inversely proportional to the radial distance from the element (similar to the inverse distance dependence of the scalar potential due to a point charge) and direction parallel to the element.

If the current in the element is now assumed to be time-varying in the manner

$$I = I_0 \cos \omega t$$

we would intuitively expect that the corresponding magnetic vector potential would also be time-varying in the same manner but with a time-lag factor included, as discussed in Sec. 8.1 in connection with the determination of the electromagnetic fields due to the time-varying current element (Hertzian dipole). To verify our intuitive expectation, we note from (8.23b) that the magnetic field due to the time-varying current element is given by

$$\begin{aligned}
\mathbf{B} = \mu\mathbf{H} &= \frac{\mu I_0\, dl \sin\theta}{4\pi}\left[\frac{\cos(\omega t - \beta r)}{r^2} - \frac{\beta \sin(\omega t - \beta r)}{r}\right]\mathbf{i}_\phi \\
&= \frac{\mu I_0\, d\mathbf{l}}{4\pi} \times \left\{\left[\frac{\cos(\omega t - \beta r)}{r^2} - \frac{\beta \sin(\omega t - \beta r)}{r}\right]\mathbf{i}_r\right\} \\
&= \frac{\mu I_0\, d\mathbf{l}}{4\pi} \times \left\{-\nabla\left[\frac{\cos(\omega t - \beta r)}{r}\right]\right\}
\end{aligned}$$

and proceed in the same manner as for the constant current case to obtain the vector potential to be

$$\mathbf{A} = \frac{\mu I_0 \, d\mathbf{l}}{4\pi r} \cos(\omega t - \beta r) \tag{10.84}$$

Comparing (10.84) with (10.83), we find that our intuitive expectation is indeed correct for the vector potential case unlike the case of the fields in Sec. 8.1! The result given by (10.84) is familiarly known as the "retarded" vector potential in view of the phase-lag factor βr contained in it.

To illustrate an example of the application of (10.84), we now consider a circular loop antenna having circumference small compared to the wavelength so that it is an electrically small antenna. Under this condition, the current flowing in the loop can be assumed to be uniform around the loop. Let us assume the loop to be in the xy plane with its center at the origin, as shown in Fig. 10.24, and the loop current to be $I = I_0 \cos \omega t$ in the ϕ direction. In view of the circular symmetry around the z axis, we can consider a point P in the xz plane without loss of generality to find the vector potential. To do this, we divide the loop into a series of infinitesimal elements. Considering one such current element $d\mathbf{l} = a \, d\alpha \, (-\sin\alpha \, \mathbf{i}_x + \cos\alpha \, \mathbf{i}_y)$, as shown in Fig. 10.24, and using (10.84) we obtain the vector potential at P due to that current element to be

$$d\mathbf{A} = \frac{\mu I_0 a \, d\alpha \, (-\sin\alpha \, \mathbf{i}_x + \cos\alpha \, \mathbf{i}_y)}{4\pi R} \cos(\omega t - \beta R) \tag{10.85}$$

where

$$\begin{aligned} R &= [(r \sin\theta - a\cos\alpha)^2 + (a\sin\alpha)^2 + (r\cos\theta)^2]^{1/2} \\ &= [r^2 + a^2 - 2ar\sin\theta\cos\alpha)]^{1/2} \end{aligned} \tag{10.86}$$

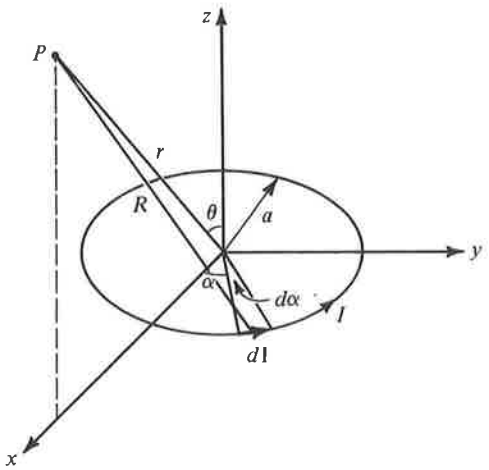

Figure 10.24. For finding the magnetic vector potential due to a small circular loop antenna.

The vector potential at point P due to the entire current loop is then given by

$$\begin{aligned}\mathbf{A} &= \int_{\alpha=0}^{2\pi} d\mathbf{A} \\ &= -\left[\int_{\alpha=0}^{2\pi} \frac{\mu I_0 a \sin\alpha\, d\alpha}{4\pi R} \cos(\omega t - \beta R)\right]\mathbf{i}_x \\ &\quad + \left[\int_{\alpha=0}^{2\pi} \frac{\mu I_0 a \cos\alpha\, d\alpha}{4\pi R} \cos(\omega t - \beta R)\right]\mathbf{i}_y \end{aligned} \tag{10.87}$$

The first integral on the right side of (10.87) is, however, zero since the contributions to it due to elements situated symmetrically about the xz plane cancel. Replacing $\mathbf{i}_y$ in the second term by $\mathbf{i}_\phi$ to generalize the result to an arbitrary point $P(r, \theta, \phi)$, we then obtain

$$\mathbf{A} = \left[\int_{\alpha=0}^{2\pi} \frac{\mu I_0 a \cos\alpha\, d\alpha}{4\pi R} \cos(\omega t - \beta R)\right]\mathbf{i}_\phi \tag{10.88}$$

Although the evaluation of the integral in (10.88) is complicated, some approximations can be made for obtaining the "radiation fields." For these fields, we can set the quantity R in the amplitude factor of the integrand equal to r. For R in the phase factor of the integrand, we write

$$\begin{aligned} R &= r\left[1 + \frac{a^2}{r^2} - \frac{2a}{r}\sin\theta\cos\alpha\right]^{1/2} \\ &\approx r\left[1 - \frac{a}{r}\sin\theta\cos\alpha\right] \end{aligned} \tag{10.89}$$

Thus for the radiation fields,

$$\mathbf{A} = \left[\int_{\alpha=0}^{2\pi} \frac{\mu I_0 a \cos\alpha\, d\alpha}{4\pi r} \cos(\omega t - \beta r + \beta a \sin\theta\cos\alpha)\right]\mathbf{i}_\phi \tag{10.90}$$

Now, since $2\pi a \ll \lambda$, or $\beta a \ll 1$, we can write

$$\begin{aligned} &\cos(\omega t - \beta r + \beta a \sin\theta\cos\alpha) \\ &\quad \approx \cos(\omega t - \beta r) - \beta a \sin\theta\cos\alpha \sin(\omega t - \beta r) \end{aligned} \tag{10.91}$$

Substituting (10.91) into (10.90) and evaluating the integral, we obtain

$$\mathbf{A} = -\frac{\mu I_0 \pi a^2 \beta \sin\theta}{4\pi r} \sin(\omega t - \beta r)\,\mathbf{i}_\phi \tag{10.92}$$

Having obtained the required magnetic vector potential, we can now determine the radiation fields. Thus from (10.77),

$$\begin{aligned}\mathbf{H} &= \frac{\mathbf{B}}{\mu} = \frac{1}{\mu}\nabla \times \mathbf{A} \\ &= -\frac{1}{\mu r}\frac{\partial}{\partial r}(rA_\phi)\mathbf{i}_\theta \\ &= -\frac{I_0\pi a^2\beta^2 \sin\theta}{4\pi r}\cos(\omega t - \beta r)\,\mathbf{i}_\theta \end{aligned} \tag{10.93}$$

From $\nabla \times \mathbf{H} = \dfrac{\partial \mathbf{D}}{\partial t} = \epsilon\dfrac{\partial \mathbf{E}}{\partial t}$, we have

$$\begin{aligned}\frac{\partial \mathbf{E}}{\partial t} &= \frac{1}{\epsilon}\nabla \times \mathbf{H} = \frac{1}{\epsilon r}\frac{\partial}{\partial r}(rH_\theta)\,\mathbf{i}_\phi \\ &= -\frac{I_0\pi a^2\beta^3 \sin\theta}{4\pi\epsilon r}\sin(\omega t - \beta r)\,\mathbf{i}_\phi \\ \mathbf{E} &= \frac{I_0\pi a^2\beta^3 \sin\theta}{4\pi\omega\epsilon r}\cos(\omega t - \beta r)\,\mathbf{i}_\phi \\ &= \frac{\eta I_0\pi a^2\beta^2 \sin\theta}{4\pi r}\cos(\omega t - \beta r)\,\mathbf{i}_\phi \end{aligned} \tag{10.94}$$

Comparing (10.94) and (10.93) with (8.25a) and (8.25b), respectively, we note that a duality exists between the radiation fields of the small current loop and those of the infinitesimal current element aligned along the axis of the current loop.

Proceeding further, we can find the Poynting vector, the instantaneous radiated power and the time-average radiated power due to the loop antenna by following steps similar to those employed for the Hertzian dipole in Sec. 8.2. Thus

$$\begin{aligned}\mathbf{P} = \mathbf{E} \times \mathbf{H} &= E_\phi \mathbf{i}_\phi \times H_\theta \mathbf{i}_\theta = -E_\phi H_\theta \mathbf{i}_r \\ &= \frac{\eta\beta^4 I_0^2\pi^2 a^4 \sin^2\theta}{16\pi^2 r^2}\cos^2(\omega t - \beta r)\,\mathbf{i}_r \\ P_{\text{rad}} &= \int_{\theta=0}^{\pi}\int_{\phi=0}^{2\pi} \mathbf{P}\cdot r^2 \sin\theta\, d\theta\, d\phi\, \mathbf{i}_r \\ &= \int_{\theta=0}^{\pi}\int_{\phi=0}^{2\pi} \frac{\eta\beta^4 I_0^2\pi^2 a^4 \sin^3\theta}{16\pi^2}\cos^2(\omega t - \beta r)\, d\theta\, d\phi \\ &= \frac{\eta\beta^4 I_0^2\pi^2 a^4}{6\pi}\cos^2(\omega t - \beta r) \\ \langle P_{\text{rad}}\rangle &= \frac{\eta\beta^4 I_0^2\pi^2 a^4}{6\pi}\langle\cos^2(\omega t - \beta r)\rangle \\ &= \frac{1}{2}I_0^2\left[\frac{8\pi^5\eta}{3}\left(\frac{a}{\lambda}\right)^4\right] \end{aligned}$$

We now identify the radiation resistance of the small loop antenna to be

$$R_{\text{rad}} = \frac{8\pi^5\eta}{3}\left(\frac{a}{\lambda}\right)^4 \tag{10.95}$$

For free space, $\eta = \eta_0 = 120\pi$ ohms, and

$$R_{\text{rad}} = 320\pi^6\left(\frac{a}{\lambda}\right)^4 = 20\pi^2\left(\frac{2\pi a}{\lambda}\right)^4 \tag{10.96}$$

Comparing this result with the radiation resistance of the Hertzian dipole given by (8.30), we note that the radiation resistance of the small loop antenna is proportional to the fourth power of its electrical size (circumference/wavelength) whereas that of the Hertzian dipole is proportional to the square of its electrical size (length/wavelength). The directivity of the small loop antenna is, however, the same as that of the Hertzian dipole, that is, 1.5, as given by (8.33), in view of the proportionality of the Poynting vectors to $\sin^2\theta$ in both cases.

In this section we introduced the magnetic vector potential as a tool for computing the magnetic fields due to current distributions. In particular, we derived the expression for the retarded magnetic vector potential for a Hertzian dipole and illustrated its application by considering the case of a small circular loop antenna. We derived the radiation fields for the loop antenna and compared its characteristics with those of the Hertzian dipole.

REVIEW QUESTIONS

10.33. Why can the magnetic flux density vector be expressed as the curl of another vector?

10.34. Discuss the analogy between the magnetic vector potential due to an infinitesimal current element and the electric scalar potential due to a point charge.

10.35. What does the word "retarded" in the terminology "retarded magnetic vector potential" refer to? Explain.

10.36. Discuss the application of the magnetic vector potential in the determination of the electromagnetic fields due to an antenna.

10.37. Discuss the duality between the radiation fields of a small circular loop antenna with those of a Hertzian dipole at the center of the loop and aligned with its axis.

10.38. Compare the radiation resistance and directivity of a small circular loop antenna with those of a Hertzian dipole.

PROBLEMS

10.23. By expansion in Cartesian coordinates, show that

$$\mathbf{A} \times \nabla V = V\nabla \times \mathbf{A} - \nabla \times (V\mathbf{A}).$$

10.24. For the half-wave dipole of Sec. 8.3, determine the magnetic vector potential for the radiation fields. Verify your result by finding the radiation fields and comparing with the results of Sec. 8.3.

10.25. A circular loop antenna of radius 1 m in free space carries a uniform current $10 \cos 4\pi \times 10^6 t$ amp. (a) Calculate the amplitude of the electric field intensity at a distance of 10 km in the plane of the loop. (b) Calculate the radiation resistance and the time-average power radiated by the loop.

10.26. Find the length of a Hertzian dipole that would radiate the same time-average power as the loop antenna of Problem 10.25 for the same current and frequency as in Problem 10.25.